2008:007 CIV

MASTER'S THESIS

Spray visualisations of gas-assisted atomisation of black liquor

Mikael Risberg

Luleå University of Technology

MSc Programmes in Engineering
Engineering Physics
Department of Applied Physics and Mechanical Engineering
Division of Energy Engineering

2008:007 CIV - ISSN: 1402-1617 - ISRN: LTU-EX--08/007--SE

Spray visualisations of gas-assisted atomisation of Black Liquor

Mikael Risberg

January 8, 2008

Preface

This report is a result of a compulsory master thesis work for the degree in master of science in engineering physics at Luleå University of Technology (LTU). The project has been going on from June to December 2007 and corresponds to 30 university points. The examiner for this project was Rickard Gebart, managing director at Energy Technology Center (ETC) in Piteå and adj. Professor at the Division of Energy Engineering, LTU. My supervisor during the work was Magnus Marklund, senior scientist at ETC.

The current project concerns atomisation of black liquor at elevated ambient pressures with the primary task to perform visualisations of the resulting black liquor spray. The obtained results will lead to a better knowledge of pressurised atomisation of black liqour. More specifically, the results will be valuable in improving modelling of black liquor gasification for use in reactor scale–up related issues.

I would to thank my supervisor Magnus at ETC for his excellent guidance and support along this project and my examiner Rikard for his advice and support in different question. Also grateful thanks to Per Gren LTU for his help with the visualisation equipment. I would also like to thank Markus Lidman, Rikard Öhman and Henry Hedman at ETC for their help and support regarding construction of different parts in this project. Many thanks to Per Carlsson at ETC for his help at the last day of practical runs and to all the employees at ETC and Chemrec for their contributions to a good working environment.

Piteå 2007-12-20

Mikael Risberg

Abstract

Black liquor gasification at high temperature is a promising alternative to the conventional recovery boiler process used in chemical pulping today. In the black liquor gasification process black liquor is atomised by a gas-assisted nozzle and sprayed into a reactor where it is directly gasified by an reaction with oxygen steam and carbon dioxide. A proper atomisation of black liquor is very important for the performance of the black liquor gasification process. The work presented in this report was performed to gain understanding and aid in optimisation of the atomisation process in the current black liquor gasification process.

The method used was spray visualisations by shadowgraphy using intensive lighting and high speed photography. The experiments were carried out in the spray test rig at the Energy Technology Centre (ETC) in Piteå and performed at elevated ambient pressures and different operational conditions.

The first part of the work was to improve the current spray test rig at ETC considering the window purging system to avoid droplets on the sight windows, the nitrogen delivering system used for atomisation and a black liquor heating and delivering system. The final setup of the spray test rig made it possible to keep the optical access windows clean, control the temperature of the atomisation gas and pump and heat the black liquor up to 115 °C.

The second part of the current work was to perform visualisations of the black liquor atomisation process in the improved spray test rig. Variables like fluid temperatures, ambient pressure, nitrogen gas flow and black liquor flow were changed in order to see how these influence the gas-assisted atomisation process of black liquor. The nozzle used in this work was a standard coaxial gas-assisted nozzle, which is not an optimised nozzle for the black liquor gasification process.

The visualisations of the resulting sprays from the current nozzle showed that black liquor does not behave like water when it is atomised. The black liquor mainly form thin ligament–shaped droplets and not spherical droplets. Based on the few result with varying black liquor temperature and dry solids content, the qualitative results showed only minor dependence from these variables in the atomisation process. Under the influence of elevated ambient pressure the black liquor spray looks more like a dense cloud of small droplets than larger more coarsely distributed droplets found in the atmospheric case.

Contents

Chapter 1

Introduction

Due to the increased energy demand in the world today and the alarming global warming it has become very important to expand the use of renewable and CO_2 neutral fuel such as Wood or biomass in general. From wood one can produce paper via e.g. chemical pulping and in Sweden 12.1 million tons of paper was produced in 2006 or about 11% of the total paper production in Europe [1]. The total energy demand from the Swedish pulp and paper industry was 78 TWh, which corresponds to 12% of the total Swedish energy balance in 2006 [2]. Because of this, the pulp and paper industry play an important role in the energy system in Sweden. By increasing the efficiency of the internal energy recovery systems in the pulp and paper mills more energy can be recovered from the mills and greatly affect the national energy balance. One way is to replace the conventional black liquor recovery boiler used in the mills chemical and energy recovery today with a black liquor gasification process. With the gasification process the total energy efficiency will increase and electricity, automobile fuels and hydrogen can efficently be produced from this process.

1.1 Black liquor recovery

In this section, the chemical and energy recovery in chemical kraft pulping are presented along with descriptions of the traditional Kraft recovery boiler process and the black liquor gasification process.

1.1.1 The chemical Kraft pulping process

In figure 1.1, the kraft pulping process is schematically described. It starts by feeding wood chips into a digester where the cellulose fibers are separated from the wood by use of white liquor. White liquor is strong aqueous solution consisting of sodium sulfate (Na_2SO_4) and sodium sulfide(Na_2S) that neutralises the organic acid and the bounding lignin in wood to separate the fibers that later become pulp. The pulp is used in the paper making process and the remaining by-products (lignin, cooking chemical, etc.) leave the digester as weak black liquor. The black liquor is then recovered to white liquor via a sequence of steps (see figure 1.1 and the following text below).

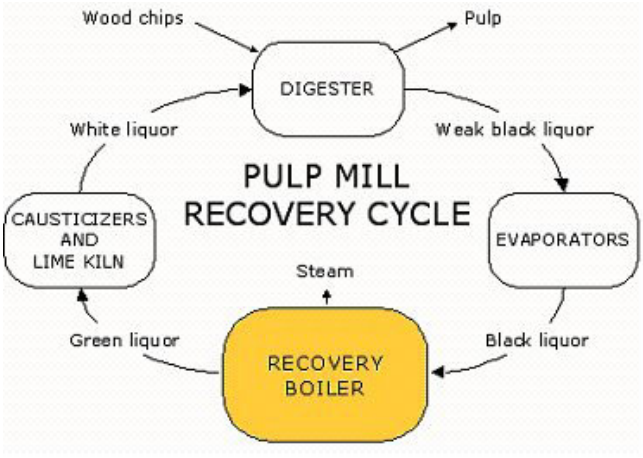

Figure 1.1: The pulping process.

1.1.2 Black liquor

Weak black liquor contains approximately 15 % solids by weight. The weak black liquor is sent through a series of evaporators to increase the solid content in order to make it suitable for combustion. The solid content in the black liquor after the evaporators is about 70-75%. The black liquor is then fired in a so called recovery boiler where it is thermochemically converted to an inorganic smelt and combustion products. The smelt is then dissolved into water to produce green liquor. The recovered energy from the recovery boiler is used internally within the mill. The green liquor then goes through a causticising process to reproduce white liquor, which then goes back into the pulping process.
Black liquor consists of several basic elements, e.g. carbon, oxygen, sodium and sulphur. The typical composition for black liquor originated from a typical Scandinavian kraft pulp mill is presented in Table 1.1.

Table 1.1: Elemental analysis in % weight of typical Scandinavian kraft black liquor solids (BLS)[3].

Element	%wt
C	34.9
H	3.4
Na	19.4
S	5.0
K	2.1
Cl	0.1
O	35.1
Others	0.0

1.1.3 Conversion of black liquor

The conversion of black liquor droplets being dispersed into the recovery boiler are mainly undergoing the following three stages: drying, pyrolysis and char conversion. The black liquor droplet first dries and evaporates its moisture. Then the droplet pyrolyse and the organic matter in the liquor degrades, forming various gaseous compounds from the volatile substances. The rate at which a droplet dries and pyrolyses is controlled by the heat transfer rate to the droplet. The resulting gases from pyrolysis are mainly H_2, CO, TRS-gases (Total Reduced Sulfur), CO_2, H_2O and some heavier carbonates [4]. The result is a swollen porous char particle that contains about 25% non-volatile organic coal material (charcoal) and about 75% inorganic salts(Na_2CO_3, Na_2S, Na_2SO_4 and corresponding potassium salts). The charcoal is the main frame and the salts are in liquid form [5]. At this stage the droplet volume might have increased by as much as 30 times the original volume [4]. This is the case for liquors coming from a sulfate kraft mill. For liquors coming from a sulfite mill, the swelling is much less [6]. The final stage is char conversion, during which mostly gas phase species react with organic constituents in the char particle, converting them into gaseous species. At the end of the char conversion stage the particle is impoverished of coal and collapse to a small droplet of smelt that consists, in the ideal case, only of inorganic material. The diameter of the droplet is then about half the original diameter [5] and consists mainly of Na_2S and Na_2CO_3 (plus some Na_2SO_4 and NaCl).

1.1.4 Recovery Boiler

Most of the recovery boilers used today are of the Tomlison type (figure 1.2). A recovery boiler acts both as a type of a high-pressure steam boiler and as a chemical reactor with reductive and oxidative zones. The black liquor is sprayed into the boiler at a temperature around 120 °C below the tertiary air register. The drying and pyrolysis conversion stage occur very quickly before most droplets fall onto a bed of char were the final conversion takes place before the inorganic smelt exits via a channel through the boiler wall and dissolves in water. The resulting combustible gases are then completely burned by the different air registers along the main wall. Steam is then produced from the combustion heat in the surrounding water pipes of the boiler, overheaters and economiser. The Tomlison boiler has served the pulping industry for about 70 years and continuous efforts have been made in order to improve its efficiency. Still, this boiler has a relatively low overall efficiency for generation of electricity.

1.1.5 Black liquor gasification

During the last decade, extensive efforts have been made to develop alternative recovery technologies based on a black liquor gasification process to supplement or replace the conventional recovery boiler. The advantage with the black liquor gasification process is that the product gas can e.g. be used in combined-cycle power generation. This technique has the potential to more than double the amount of net electrical energy for a Kraft pulp mill compared to an ordinary recovery boiler with a steam turbine [7]. As an alternative, this technique also has the potential to convert the produced synthetic gas to a motor fuel such as DME (dimethylether), methanol or synthetic diesel.

During the last decade three different black liquor recovery processes have been under development:

- Partial combustion in short–residence–time entrained–flow reactors

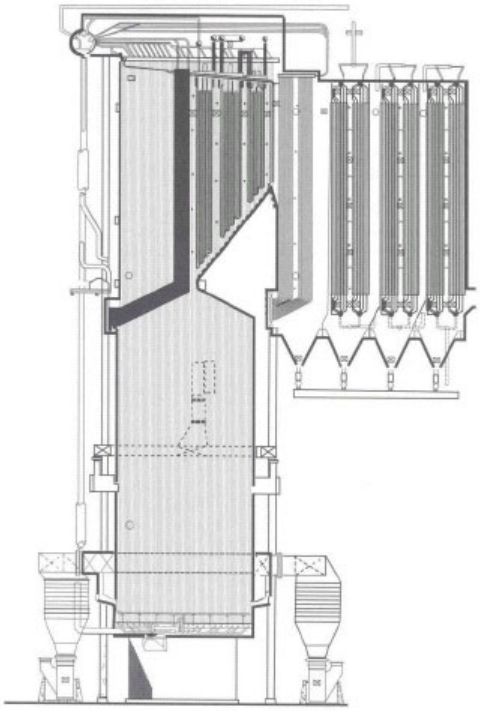

Figure 1.2: Tomlinson recovery boiler.

- Partial combustion in long–residence–time fluidised beds
- Steam gasification in indirectly heated fluidised beds

The most promising alternative so far is the Chemrec pressurised black liquor gasification process (PBLG), which is of the first kind in the list above. In Piteå, a pressurised black liquor gasification development plant (DP1) has been constructed by Chemrec at Energy Technology Center (ETC). In figure 1.3 a schematic drawing of the development plant is presented. At the top of the reactor black liquor is dispersed into the hot reactor cavity together with an under–stoichiometric amount of oxygen by use of a spray burner nozzle. The resulting droplet size is about 100–300 micrometer compared to 1–5 millimeter for a conventional recovery boiler. The amount of oxygen supplied to the reactor is important and should be as small as possible since it is favorable with a high heating value on the resulting gas. To get high enough residence times for the black liquor droplets to prevent unacceptable organic material in the resulting smelt it is important to have a favorable spray pattern. After the reactor the products reach the quench where the different products separate into gas and smelt. The gas raise up to the top of the quench and passes through a counter–current condenser where some volatile substances and steam are condensed, and pumped back to the quench. The gas then goes on to further cleaning processes before it can be used in gas turbines or be converted to motor fuel. The dissolved smelt in the quench is being washed and goes back into the recovery cycle as green liquor.

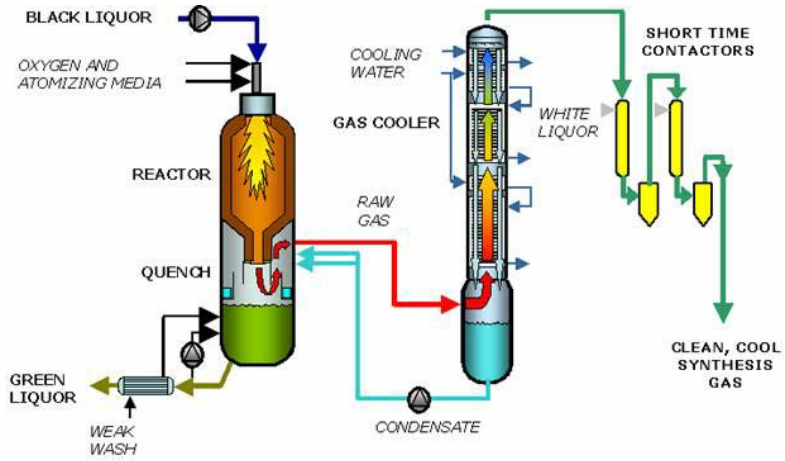

Figure 1.3: Schematic drawing of the CHEMREC black liquor gasification process.

1.2 Atomisation

The atomisation process is when a volume of liquid is breaking up into multiplicity of small drops. This process is one in which a liquid jet or sheet is disintegrated by the kinetic energy of the liquid itself, or by exposure to high-velocity air or gas, or as a result of mechanical energy applied externally through a rotating or vibrating device [8]. The random nature of atomisation results in a wide spectrum of drop sizes. Examples of different types of atomisers are pressure atomisers and rotary atomisers which eject the liquid at high velocity into a slow-moving stream of air or gas. In the black liquor gasification process, slow moving black liquor is exposed to a high velocity gas stream. This latter method is known as air or gas assisted atomisation.

1.2.1 Physical properties of Black Liquor

Properties of black liquor like dry solids content, viscosity, density and surface tension are difficult to obtain as they are both functions of the liquor composition and process conditions. However, these properties are very important in understanding the atomisation of black liquor. Dry solids content is the mass of a dried liquor sample as a percentage of the original sample mass. This property is one of the most significant factors to determine other properties. Density is an important property for the flow characteristics. The density will increase as the dry solids content increase and it is also dependent of the temperature. A higher temperature gives a lower density [9]. Surface tension of black liquor is dependent on the liquor composition, dry solids content ,temperature [9] and the time after surface formation. For example surface tension generally decreases as the temperature increase and decrease with time after surface formation [10]. The viscosity depends on a number of factors, but most affected by the dry solids content and temperature. By increasing the temperature the viscosity will decrease but a higher dry solids content will increase the viscosity [11]. In figure 1.4 it can be seen how the viscosity depends on temperature and dry solids content. The viscosity showed in 1.4 is from a paper mill that uses only hardwood. In this work, black liquor was taken from a pulp mill that uses a combination of 70 percent hardwood and 30 percent softwood. A mixed black liquor with both hardwood and softwood will decrease the viscosity

slightly compared to a black liquor with only hardwood [10].

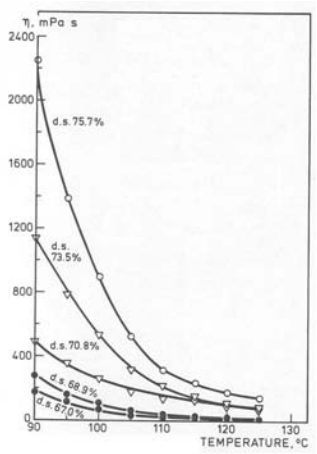

Figure 1.4: Viscosity of five different black liquor samples as a function of temperature [11].

1.2.2 Earlier work on black liquor sprays

Some earlier work has been made on black liquor spray visualisation but most of them is with a splash plate nozzle used in a conventional recovery boiler. However some work has been done with a gas–assisted nozzle, e.g. the work by Mackrory and Baxter [12] and Mackrory thesis work [13]. They used a gas–assisted nozzle and visualised with high speed photography. Mackrory and Baxter found that the black liquor forms long, thin ligaments rather than droplets, which can be seen in figure 1.5. Loebker and Empie [14] have also done some work based on effervescent atomisation where air is mixed with the black liquor feed at some point upstream of the nozzle orifice so that a bubbly two–phase flow is produced. In their work they used a corn syrup and water mixture as model fluid.

1.3 Spray test rig

For an optimal function of black liquor gasification it is very important to understand how the black liquor spray behaves and looks. Both the velocity and droplet size can be optimized with respect to an efficient droplet conversion in the black liquor gasification process. At the Energy Technology Centre in Piteå a Spray test rig has been developed [15] in order to be able to characterise and optimize the spray of black liquor in the gasification process. In this section the designs of the main parts in the spray test rig are presented.

1.3.1 Pressure vessel

The spray test rig is made up by a pressure vessel that is 5600 mm in total height and has a diameter of 500 mm. The vessel is tested and approved for a pressure of 15 bar and is made of stainless steel (SS2342) to prevent corrosion from black liquor. The bottom

Figure 1.5: Spray visualisation of gas–assisted black liqour atomisation done by Mackrory [13].

of the vessel can also be used as a reservoir tank with a volume of 400 l. Nitrogen gas is used to build up the pressure in the vessel and a pressure control valve is used to regulate the pressure. For security reason also a pressure release valve is mounted at the vessel to be able to quickly release the pressure if it exceeds its design pressure.

1.3.2 Optical Access Windows

Four optical access windows are placed approximately 500 mm from the top of the vessel. The windows are located at $0°$, $106°$, $210°$ and $270°$ (figure 1.7) to satisfy the demands of Phase Doppler Anemometer measurement. The window glass (Figure 1.8) is quartz glass with quality SILUX (200 mm in diameter and 50 mm thick). SILUX satisfies the demands of optical quality for measurement of droplets and sprays. The glasses are tested to withstand pressures up to 15 bar.

1.3.3 Spray lance traversing system

On top of the vessel a lance traversing system is mounted in order to the traverse the spray nozzle in the vertical direction up and down and rotate it (figure 1.9). This system enables measurements in a large part of the spray and easy change to a different nozzle. The lance is the same as the one Chemrec use in their DP-1 pilot plant, which make it easy to test different nozzles from the DP-1 plant.

1.4 Visualisation techniques

To optimize the spray pattern it is important to know how black liquor behaves and looks when it is sprayed. Following is a presentation of high speed photography and visualisation techniques that can be used in spray visualisations.

Figure 1.6: Spray test rig at Energy Technology Centre.

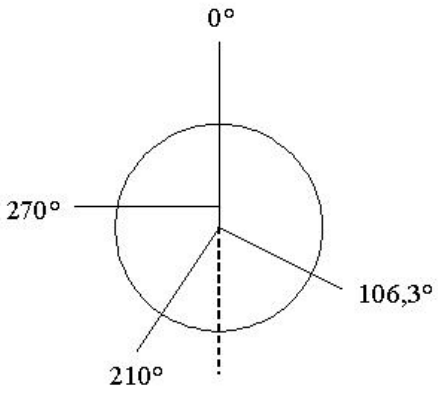

Figure 1.7: Placement of optical access windows.

1.4.1 High Speed Photography

A general definition for high speed photography could be described as recording optical or electro–optical information fast enough for an event to be evaluated with a temporal resolution which satisfies the experimenter [16]. High speed photography has two major benefits. First, it enables the observation and recording of events in which the movement is normally too rapid to be followed by the naked eye. Furthermore, it gives the power to manipulate time; events can be speeded up or slowed down from their natural occurrence rate when the record is reproduced. This is a major advantage as the event can be played back repeatedly at a rate which can be followed by the naked eye, until all the information required has been obtained either by simple observation or by detailed analysis [17].

Figure 1.8: Quartz glass for Optical Access Windows.

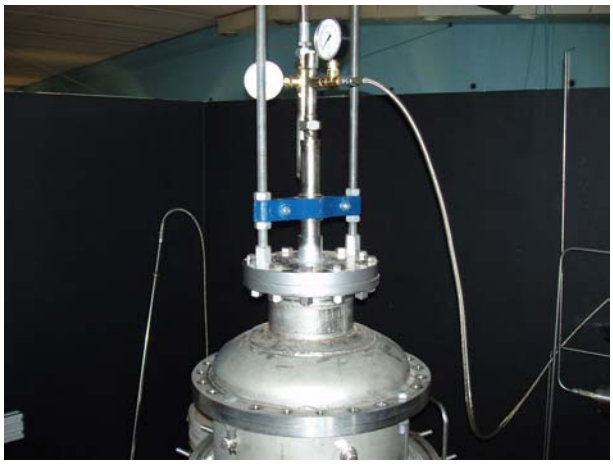

Figure 1.9: Spray lance traversing system.

Types of lighting

In high speed photography different types of lighting are used from sunlight to super radiant light sources. In table 1.2 some different types are listed and the typical duration time for each type. What types of lighting to choose are dependent of the application in which the high speed photography is used in. For example it might be preferred to use a pulsed laser with high intensity to photograph sprays with small droplets and high velocity.

Applications of high speed photography

High speed photography is nowadays used in almost all branches of scientific research. The use is growing steadily as exposure times become shorter, framing rates become faster and resolution and image quality improves [17]. The development of digital cameras also has improved the use of high speed photography. In table 1.3 some application

Table 1.2: Types of lighting used for high speed photography[17].

Source	Typical duration (s)
Sunlight	Continuous
Tungsten filament lamps of various types	Continuous
Arc sources	Continuous
Flash bulbs	$0.5 - 5 * 10^{-3}$
Electronic flash	$10^{-3} - 10^{-6}$
Argon bomb	$10^{-6} - 10^{-7}$
Electric spark	$10^{-6} - 10^{-9}$
X–ray flash	$10^{-7} - 10^{-9}$
Pulsed laser	$10^{-6} - 10^{-12}$
Super radiant light sources	10^{-9}

of high speed photography is listed.

Table 1.3: Different field of application of high speed photography [17].

Fluid flow and combustion research
Auto and armament research
Machining and tool design
Manufacturing processes
Physical and chemical processes
Sporting and physiological studies
Behaviour and movement of animals, birds and insects
Lighting and electrical engineering research
Medical research
Astrophysics research
Accident research
Racing timing
Transport and vehicle research
Materials research
Atomic energy research
Educational studies
Advertising and entertainment

1.4.2 Particle Image Velocimetry (PIV)

PIV is a whole field measurement technique that takes two pictures shortly after each other and calculates how long each particle has travelled within this time. From the known time between the pictures and the distance that the particle has travelled the velocity of the particle can be calculated. To avoid a blurred image for fast flows a pulsed laser can be used. Laser pulses from a Nd.Yag laser can be about 10-20 ns. The other reason for using a laser is that laser light can be focused into a thin plane so that only particles on that plane are imaged. In PIV a special camera must be used that can store the first picture and than be ready for exposure of the second picture fast enough. A illustration of a PIV system is showed in figure 1.10. [18]

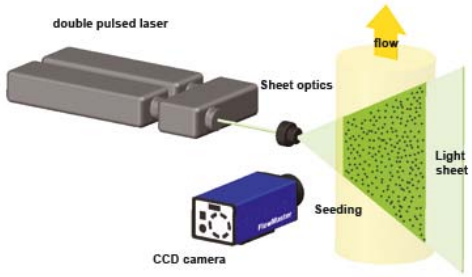

Figure 1.10: PIV technique [18].

1.4.3 Shadowgraphy

In this technique the object is backlighted with a light source and a camera acquires the shadow of object. In the case of a particle flow, a short light flash and a synchronisation device are used to freeze the particle motion or a continuous light source and a camera with a short exposure time can also be used. An illustration of a shadowgraphy set–up is showed in figure 1.11 [19].

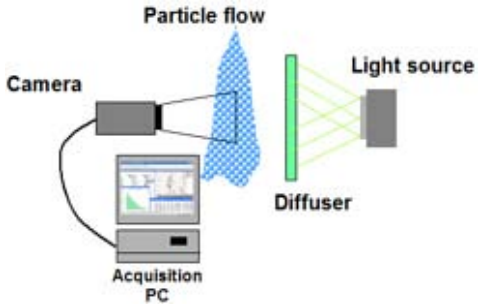

Figure 1.11: Shadowgraphy technique [19].

1.5 Introduction to CFD

In this section a introduction to Computational Fluid Dynamics (CFD) are presented. CFD is a widely used numerical method to solve fluid dynamics related problems. The solution procedure starts with choosing a computational domain from the geometry (CAD) that is to be investigated. The computational domain is then divided into small connected elements called cells forming a mesh. It is very important to have a mesh of high quality to obtain an accurate solution. Then the boundary conditions are specified on each face of the domain and the type of fluid and fluid properties are specified (the commercial code Ansys CFX that was used for this thesis has a built in property database for most of the common fluids). After that some initial conditions are specified for each cell and numerical parameters and solutions algorithms are selected. Then the linearised and discretised equations of the fluid flow problem are solved iteratively in the CFD solver with the initial conditions as an initial guess. In CFD simulations residuals never becomes identically zero but will hopefully decrease for each iteration.

When the residuals are below a certain limit the solution is defined as converged. The converged solution can then be analysed by the use of a postprocessor.

1.6 Thesis background and objectives

In most modelling work on black liquor gasification e.g Marklund [3] it is assumed that the black liquor spray is made up of spherical droplets with a certain size distribution. However, recent experimental work by Baxter and Mackrory [12] have shown that black liquor atomised by a gas-assisted nozzle form long and thin ligaments rather than droplets when atomised with high speed gas. If this is generally the case, the modelling approach must be modified. However, in their work they used a relatively low amount of atomisation gas compared to what is believed to be needed in the BLG process. Hence, it is of interest to investigate how the atomisation will change when the amount of atomisation gas is increased. Furthermore, it is of interest to find out how gas-assisted atomisation of black liquor is influenced by elevated ambient pressure. The main objective with the current thesis was therefore to study the atomisation and spray formation resulting from gas-assisted atomisation of black liquor when atomised with high speed gas at elevated pressures. Specifically, the work was aimed at providing:

- A functional spray test rig that is able to spray water or black liquor at high momentum flux ratios and at different ambient pressures up to 15 bar.
- An appropriate visualisation techniques suitable for studies of black liquor gasifier sprays.
- Spray visualisations of water and black liquor sprays using appropriate visualisation technique in the spray test rig at the Energy Technology Centre.

Chapter 2

Method

In order to perform visualisations of black liquor atomisation in the existing spray test rig some improvement had to be made. In this section the different improvements are presented. First, the construction of the window purge system is presented followed by the improvements in the nitrogen delivering system. Then the design and construction of the black liquor heating and delivering system are presented. A presentation of the visualisation technique used in the current project is also presented. Finally, the different visualisation cases of atomisation with water and black liquor are presented together with a description of the nozzle used in this work.

2.1 Experimental setup

The used spray test rig mainly consists of a pressure vessel with optical access ports and a nitrogen delivery system. The construction of the pressure vessel was made by Karlsson and Westerlund [15] in their master thesis work at ETC. Some improvement had be made in the test rig in order for it to be used, e.g. a window purging system to prevent droplets to end up on the sight windows. The nitrogen delivery system had to be equipped with a mass flow meter and controller, and a nitrogen heater to heat the gas. A black liquor heating and delivery system had to be constructed to be able to spray black liquor in the test rig.

2.1.1 Window purge system

To prevent droplets from ending up on the optical access windows, a window purging system had to be designed. First, some qualitative tests of some different conceptual models made of styrofoam were performed. After that, a purging system made out of stainless steel was constructed and tested experimentally. In addition, a CFD model of the purging system was also created.

Qualitative test of windows purging system

Initially, different types of window purging systems with models made of styrofoam were investigated qualitatively. Se figure 2.1 for some example of the models and figure 2.2 for a picture where the model is mounted in the spray rig. From the qualitative tests the conclusion that a straight tube is better then some sort of cone and the diameter of

the tube should not be larger than 110 mm in order to prevent the droplets to reach the window.

Figure 2.1: Window purging system models made out of styrofoam.

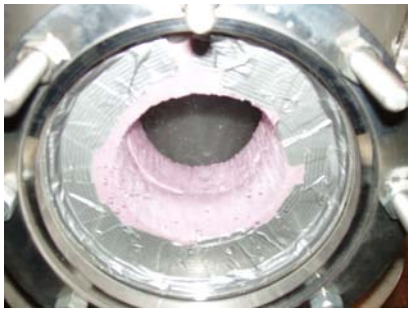

Figure 2.2: Window purging system models mounted in one of the optical access ports in the spray test rig.

CFD simulation of window purging system

In this project, a two–phase modell (water droplets and air) for a the current window purging system have been investigated with the commercial CFD software CFX–11.0 from Ansys. The results for the CFD calculations are presented in the section results of CFD simulation.
Three different cad geometries of the window purging system with different number of air inlets((one, two and four) were created (see figure 2.3). The geometries were cut in half due to a symmetry assumption. Three meshes were created based on the different geometries with inflated boundaries at the wall. The meshes are constructed with Ansys Workbench. In table 2.1 the mesh statistics for the different meshes are shown and in figure 2.4 the mesh with one inlet i showed.

Table 2.1: Mesh Statistics.

	1 inlet	2 inlet	4 inlet
Nodes	95335	95704	92263
Elements	432782	433499	431651

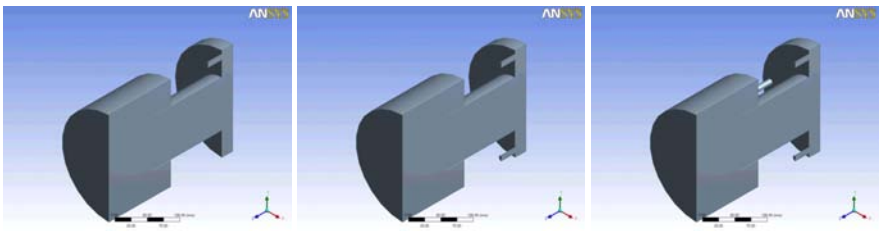

(a) One inlet. (b) Two inlet. (c) Four inlet.

Figure 2.3: Geometri of window purging system.

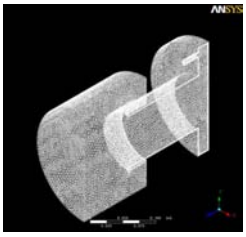

Figure 2.4: Mesh of window purging system with 1 inlet.

Six different boundary conditions are applied to the mesh (see figure 2.5). Below follows a description for each of the specified boundary conditions:

Inlet: Mass flow inlet type with an air flow of 0.0014 kg/s that correspond to 71 l/min (0 °C and 1 atm) for the symmetry solution (142 l/min for the whole purging system).

Glass: The boundary type for the glass is a wall with no slip condition.

Wall: The boundary type for the wall is a wall with no slip condition.

Opening: The boundary type for the opening is an opening and the relative static pressure is set to 0 bar.

Opening2: The boundary type for the opening2 is an opening with particle injected with a velocity of 10 m/s. The size of the particles is 100,125,150,175,200,250 and 300 um. 1000 particles of each size are injected. The relative static pressure is set to 0 bar.

Symmetry: The boundary type of symmetry is a symmetry plane. The symmetry plane reduce the computational cost and allow smaller elements that provide better accuracy in the results.

Construction of window purging system

From the qualitative tests and models simulations a purging system of stainless steel was constructed. In figure 2.6 the purging system is shown.

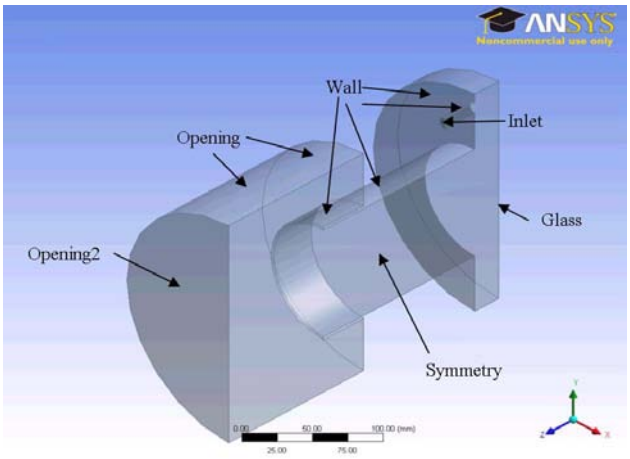

Figure 2.5: Boundary conditions.

Figure 2.6: Window purging system for mounting in the spray test rig.

Experimental set up for the window purging system

Practical experiments were performed on the final window purging system at atmospheric conditions. Six different cases were evaluated with the purging system and shown in table 2.2. The results from this part are presented in the section of experimental results. In table 2.2 the flow rate is the liquid flow through the nozzle in l_n/min, where the l_n/min is the liquid flow rate at atmospheric pressure and 0 °C. The lance position is how far the nozzle tip is from the top of the vessel. Furthermore, the inlet is if the inlet of nitrogen gas are above (up) or below (down) the straight tube into the vessel. The nitrogen gas flow rate for these cases was controlled with a ball valve that was opened fully. Each case was run five minutes before the results were obtained.

2.1.2 Nitrogen delivering system

The nitrogen gas for use in the spray test rig come from a nitrogen tank supply hosted and controlled by Chemrec. In order to heat the cool nitrogen gas coming from the evaporating unit in the tank supply system an electric 9kW heater was installed. Also two mass flow meters and controllers for nitrogen gas were installed to be able to control the flow of nitrogen gas to the spray test rig. In figure 2.7 a flow chart of the nitrogen

Table 2.2: Different Experimental Setup.

Case	Flow (l_n/min)	Lance position (mm)	Inlet
1	9.0	45	Up
2	13.8	45	Up
3	9.0	100	Up
4	13.7	100	Up
5	9.0	100	Down
6	14.1	100	Down

delivery system is presented.

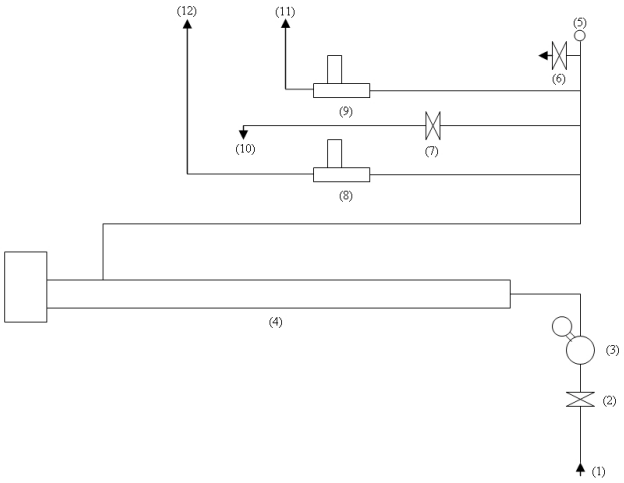

1. Nitrogen inlet from the nitrogen tank at Chemrec
2. Ball valve to be able to shutdown the nitrogen flow
3. Pressure reducing valve to control the pressure of the system
4. Nitrogen gas heater to heat the gas to about 20 °C
5. Pressure meter
6. Ball valve to be able to leak the nitrogen gas out and not to the spray test rig
7. Ball valve to open or close the gas flow to the window purging system
8. Mass flow meter and controller to be able to control the amount of gas from 0 l_n/min to 100 l_n/min
9. Mass flow meter and controller to be able to control the amount of gas from 0 l_n/min to 2500 l_n/min
10. Gas pipe to the window purging system
11. Gas pipe to the nozzle for the atomisation gas
12. Gas pipe to the nozzle for a secondary atomisation flow

Figure 2.7: Flow chart of the nitrogen delivering system with a description of each of the items numbered in the flowchart.

Gas heater

An electric heater manufactured by Backer with the power of 9 kilowatt was installed to be able to heat the nitrogen gas from about $-30\,^{\circ}$C to about $20\,^{\circ}$C. Some heater specifications are listed in table 2.3 and a picture of the heater is shown in figure 2.8.

A power calculation was made to determine the power need of the gas heater. The

Table 2.3: Nitrogen gas heater specifications.

Name	EHU9KW-PN25
Power (kW)	9
Voltage (V)	380/220
Pressure class (Bar)	PN25

Figure 2.8: 9kW nitrogen gas heater.

calculation was based on a flow rate of 2500 l_n/min, which correspond to a mass flow rate of $\dot{m}$ = 2.825 kg/min, a temperature increase of dt = $50\,^{\circ}$C, C_p = 1.042 kJ/kg–K for nitrogen gas. Inserting into equation 2.1 gives Power $\dot{W}$ = 2.45 kW. From this calculation it was concluded that the 9kW electric heater should be able to heat the nitrogen gas by more than $50\,^{\circ}$C.

$$\dot{W} = \dot{m} c_p dt \tag{2.1}$$

Mass flow meters

Two mass flow controllers 5853S from Brook instruments were installed in order to measure and control the flow of nitrogen gas to the spray test rig. One controller is able to control the flow rate from 0 to 2500 l_n/min for the main atomisation gas and the other from 0 to 100 l_n/min for a possible second stream of atomisation gas. The mass flow controllers consist of a thermal mass flow sensor and an integrally mounted control valve module with which stable gas flows can be achieved [20].

Thermal mass flow meters are based on an operational principle that states that the rate of heat absorbed by a flow stream is directly proportional to its mass flow rate. As molecules of a moving gas come into contact with a heat source, they absorb heat and

thereby cool the source. At increased flow rates, more molecules come into contact with the heat source, absorbing even more heat. The amount of heat dissipated from the heat source in this manner is proportional to the number of molecules of a particular gas (its mass), the thermal characteristics of the gas, and its flow characteristics.
Constant temperature thermal mass flow meters such as those produced by Brooks Instrument, requires two active sensors that are operated in a balanced state. One act as a temperature sensor reference; the other is the active heated sensor. Heat loss produced by the flowing fluid tends to unbalance the heated flow sensor and it is forced back into balance by the electronics. With this method of operating the constant temperature sensor, only the skin temperature is affected by the fluid flow heat loss. This allows the sensor core temperature to be maintained and produces a very fast response to fluid velocity and temperature changes. Additionally, because the power is applied as needed, the system has a wide operating range of flow and temperature. The heated sensor maintains an index of overheat above the environmental temperature sensed by the unheated element. The effects of variations in density are virtually eliminated by molecular heat transfer and sensor temperature corrections [21].

2.1.3 Black liquor heating and delivering system

To be able to spray black liquor in the test rig the liquor has to be heated up to $100-120\,^{\circ}$C. In order to do so a heat and pump system had to be constructed. In figure 2.9 a flow chart of the heat and pump system is presented. The system works in the way that the black liquor is stored in a vessel, and the vessel is heated with two vessel heaters to about $100\,^{\circ}$C. After that the black liquor will flow into a peak heater with 10 electrical heaters that will heat the liquor up to about $115\,^{\circ}$C. The liquor will then be pumped from the bottom of the heater by an eccentric screw pump either back to the top of the heater or to a lobe rotor pump. The lobe rotor pump will then pump the liquor to the spray test rig.

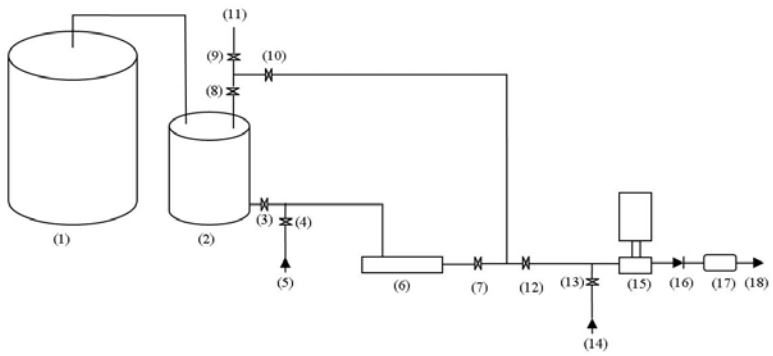

1. Black liquor vessel with heaters
2. Peak heater with 10 electrical heaters
3. Ball valve
4. Ball valve
5. Inlet for water to flush the system
6. Eccentric screw pump for recirculation of black liquor or to feed the lobe pump with black liquor
7. Ball valve
8. Ball valve
9. Ball valve
10. Ball valve
11. Inlet for water to flush the system or outlet for air when the peak heater is filled
12. Ball valve
13. Ball valve
14. Inlet for water to flush the system
15. Lobe pump
16. Back valve to prevent the black liquor or the nitrogen gas to flow back into the black liquor system
17. Flow meter to measure the flow of black liquor
18. Pipe for black liquor to the spray test rig

Figure 2.9: Flowchart for the black liquor heat and pump system with description of each item in the flowchart.

Vessel

To store the black liquor a 200 litre barrel was used. The barrel was heated with one 2000 W oil drum heater. In this stage the black liquor was heated to 90 °C to 100 °C. In figure 2.10 two of the barrels along with heaters are shown.

Figure 2.10: Storage and heating of black liquor.

Peak heater

To be able to heat the black liquor from about 100 °C to 110 – 120 °C a peak heater was constructed. The peak heater consists of a stainless steel vessel and 10 electric heaters with the power of 6 kW each. To prevent the black liquor from intensive boiling locally the electric heaters were configured so that the total power was 7 kW for the 10 heater. An eccentric screw pump was also used to circulate the black liquor from the bottom of vessel to the top. See figure 2.11 for a picture of the peak heater.

Figure 2.11: Peak heater for black liquor.

Eccentric screw pump

To feed the lobe rotor pump and circulate the black liquor an eccentric screw pump was used. The pump is a NEMO–Pump N 20 from Netzsch. This pump can handle temperatures from $-40\,^{\circ}$C to $200\,^{\circ}$C and pressures up to 6 bar. The principle of an eccentric screw pump is that a rotor is turning inside a stator to produce a flow directly related to the revolutions per minute [22]. In table 2.4 some specifications of the used pump are listed and in figure 2.12 the pump is shown.

Table 2.4: Pump specifications for the eccentric screw pump.

Name	NEMO–Pump N 20
Port Size (inches)	1 1/4
Maximum Flow (/min)	87
Maximum diff pressure (bar)	6
Maximum Speed (rpm)	3000
Weight (bareshaft) kg	9.5
Temperature degress celcius	-40 to +200
Viscosity cP	1 to 1 million

Figure 2.12: N 20 excenterscrewpump.

Lobe rotor pump

To pump the black liquor fed by the eccentric screw pump to the nozzle the existing pump at the spray test rig was chosen. The pump is a LH3 rotary lobe rotor pump developed by JABSCO (figure 2.13). The parts of the pump that are in contact with the liquor is made from low carbon stainless steel to prevent corrosion from the black liquor. The maximum working pressure is 15 bar but if the temperature of the liquor is $140\,^{\circ}$C the maximum pressure must be restricted to 10 bar. In table 2.5 some pump specifications are listed. The principle of operation for a lobe rotor pump is that two rotors turn in an opposite direction and fluid goes into the pump from an inlet port and fills the space between the rotors. This fluid is carried around the outside of the rotors

and is forced out of the discharge port as the rotor lobes mesh together. Figure 2.14 illustrates this principle [23].

Figure 2.13: LH3 rotary lobe pump [23].

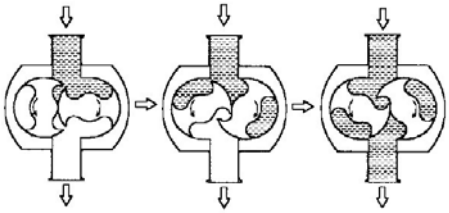

Figure 2.14: Principle of a lobe pump [23].

Flow meter for water/blackliquor

To measure the flow of water or black liquor an induction flow meter FLONET FR 2014 from Elis Plzen a.s was installed (figure 2.15). Minimum and maximum flow rate for this meter are 0.008 l/s and 0.8 l/s, respectively. The function of an induction flow meter is based on Faraday's induction law. The meter sensor consists of a nonmagnetic and nonconductive tube with two embedded measuring electrodes to pick up the induced voltage. To create an alternating magnetic field, two coils are fitted onto the tube in parallel with the plane defined by the active parts of the measuring electrodes. Now if a conductive liquid flows across magnetic field **B**, voltage **U** will appear on the measuring electrodes proportional to the flow velocity **v** and the conductor length **I**. As the magnetic flux density and distance between the electrodes are constant, the induced voltage is proportional to the liquid flow velocity in the tube. The value of the volume flow rate can then be readily determined as a product of the flow velocity and square section of the tube, i.e. **Q = c x S** [24].

Table 2.5: Pump specifications for the lobe pump.

Name	Hy Line LH3
Port Size (inches)	1
Displacement (litre/min)	3.5
Maximum Flow (litre/min)	52
Maximum diff pressure (bar)	15
Maximum Speed (rpm)	1500
Dimensions LxBxH mm	213 x 192 x 166
Weight (bareshaft) kg	8
Temperature °C	-30 to +140
Viscosity cP	1 to 1 million

Figure 2.15: Flow meter FLONET FR 2014.

2.2 Visualisation techniques

The visualisation of black liquor atomisation was made with a high speed camera and backlighting usually referred to as shadowgraphy. See figure 2.16 for the visualisation setup where (1) is the camera and (2) is two light sources.

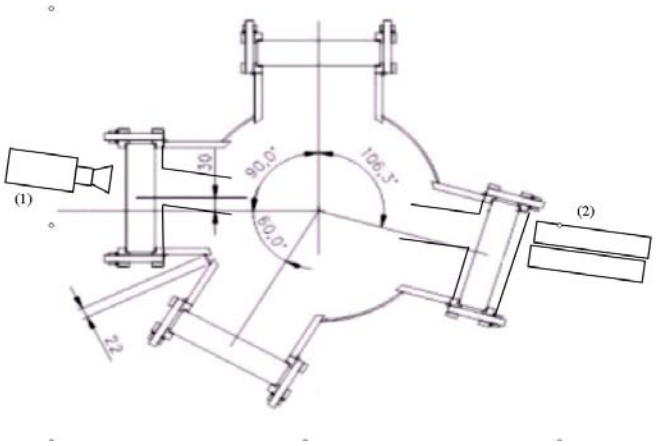

Figure 2.16: Visualisation setup.

2.2.1 Camera

A MotionPro X3Plus cmos camera (figure 2.17) from Redlake was used for the high speed photography of the spray. Motionpro X3Plus is a mono camera with resolution up to 1280x1024 pixels with a frame rate of 2000 frames per second. By decreasing the vertical resolution the frame rate can be increased up to 128.000 frames per second for a vertical resolution of 16 pixels. The camera allows for a global shutter time down to 1μs to be able to avoid motions blur for fast moving objects. The lenses that were used was a 55 mm Micronikkor for the first cases (case 1 to 6) or a 110 mm zoom objective from Canon together with a 450 mm close up lens from Canon for the latter cases (case 7 to 12).

2.2.2 Lighting

Two COOLH Dedocool tungsten light heads were used to light the droplets from behind. These lights use a low wattage, low voltage lamp in combination with an optical system and a special reflector, which concentrates an intense amount of light over a concentrated area [25]. Also a diffusor is used between the optical access window and the lightings. See figure 2.18 for setup of the lighting at the spray test rig.

2.2.3 Window purging system for shadowgraphy

To be able to use backlighting a new window purging system had to be constructed. In figure 2.16 the new window purging system is shown as two opposite tubes in an angle with the inside of the port windows. In figure 2.19 a picture of the new purging system is presented.

Figure 2.17: MotionPro X3Plus camera.

Figure 2.18: COOLH Dedocool Tungsten Light Head with a diffusor between the optical access window and the lighting.

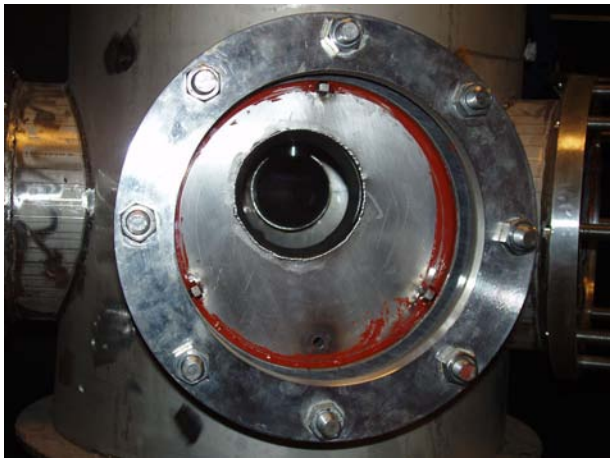

Figure 2.19: New window purging system constructed and mounted.

2.3 Spray visualisation

In this section the different spray visualisations as atomisation runs are presented both for water and black liquor. First, a presentation of the used nozzle at the visualisation is presented.

2.3.1 Nozzle

The used nozzle is of a twin–fluid coaxial convergent air–assisted type. See figure 2.20 for schematics of the nozzle. The nozzle exit for the liquid has a diameter of 9 mm and the upstream diameter for the liquid inside the nozzle before the contraction is 12.7 mm. The gap for the surrounding annular gas exit is 0.65 mm and the annular contraction area ratio (ratio of entrance to exit area of the contraction) for the gas flow is 16.5. Furthermore, the liquid to gas nozzle exit area ratio is equal to 2.67. The nozzle in this work is standard nozzle and is not optimised for the black liquor gasification process.

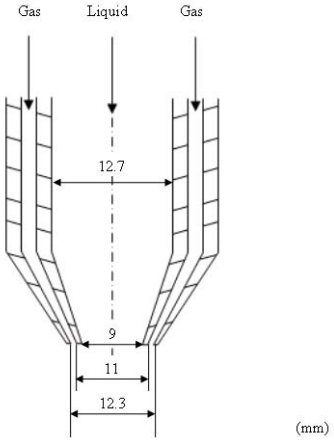

Figure 2.20: Schematics of the nozzle.

2.3.2 Water

One case with water was visualised to be able to compare with the black liquor runs. In table 2.6 the data for the water run is presented, where the l_n/min is the liquid flow rate at atmospheric pressure and 0 °C. Also the momentum flux ratios M between the gas and liquid are shown in the table. The momentum flux ratio can be expressed as:

$$M = \frac{\rho_g U_g^2}{\rho_l U_l^2} \tag{2.2}$$

Where ρ_g is the density of the gas, ρ_l density of the liquid, U_g the velocity of the gas and U_l the velocity of the liquid.

2.3.3 Black liquor

In table 2.7 the data for different cases for black liquor atomisation runs are presented. The different variables that were studied were the temperature of black liquor and flow

Table 2.6: Water run data. M is calculated based on a choked flow.

Case	Pressure (bar)	Liquid flow (l_n/min)	Gas flow (l_n/min)	M	Temperature (°C)
1	1.013	4.9	441	90	50

rate of black liquor and the flow rate of nitrogen gas. The pressure was also varied for some cases. The resulting momentum flux ratio M (see eq 2.2 above) between the gas and liquid are also shown in the table. In case 1 to 10 M is calculated based on the assumption of a choked compressible flow. In case 11 to 13 the flow is assumed to be incompressible. The temperature of the nitrogen gas was about $16-20\,^{\circ}\mathrm{C}$ for every run and the percent dry solids in the black liqour (DS) was 75.2% for case 1 to 6 and 70.2 for case 7 to 13. The viscosity is also presented, however the viscosity is taken from a diagram from the thesis of Soderhjelm [10] and is not measured specific for the black liquor in this work.

Table 2.7: Black liqour runs data.

Case	Pressure (bar)	Liquid flow (l_n/min)	Gas flow (l_n/min)	M	Temperature (°C)	DS %	Viscosity (m Pa)
1	1.013	4.9	441	60	102	75.2	500
2	1.013	4.9	588	80	102	75.2	500
3	1.013	4.9	735	100	102	75.2	500
4	1.013	7.3	992	60	102	75.2	500
5	1.013	7.3	1322	80	102	7 5.2	500
6	1.013	7.3	1652	100	102	75.2	500
7	1.013	4.9	441	60	112	70.2	150
8	1.013	4.9	735	100	112	70.2	150
9	1.013	7.3	992	60	112	70.2	150
10	1.013	7.3	1652	100	112	70.2	150
11	5	7.3	1652	72*	112	70.2	150
12	10	7.3	1652	36	112	70.2	150
13	10	7.3	2140	60	112	70.2	150

*Difficult to determine if the flow is compressible or incompressible for this case

Chapter 3

Results

In this chapter the results for the window purging system are presented. Followed by a presentation of the result for the water sprays visualisation. Finally, the results from the different cases of black liquor spray visualisations are presented.

3.1 Window purging system

In this section the results from the CFD simulation and experimental results for the window purging system are presented.

3.1.1 CFD results

In this section the results from CFD-simulation of the window purging system are presented. In figure 3.1 the results for a single inlet of gas into the window cavity are presented. In the presented figures it can be seen that in the lower part of the tube droplets enter relatively easy even for small droplets with a diameter of 125μm but they do not reach the window. However, for droplets with a diameter larger than 150μm they reach the window. In figure 3.2 the results for two gas inlets of gas into the window cavity are presented. For small droplets with a diameters up to 125μm this purging system work very well, but the droplets with a larger diameter than 150μm are still reaching the window. In figure 3.3 the results for 4 gas inlets into the cavity are presented and here it can be seen that this configuration also purge droplets with diameters up to 150μm. Droplets with a diameter of 175μm still reach the window.

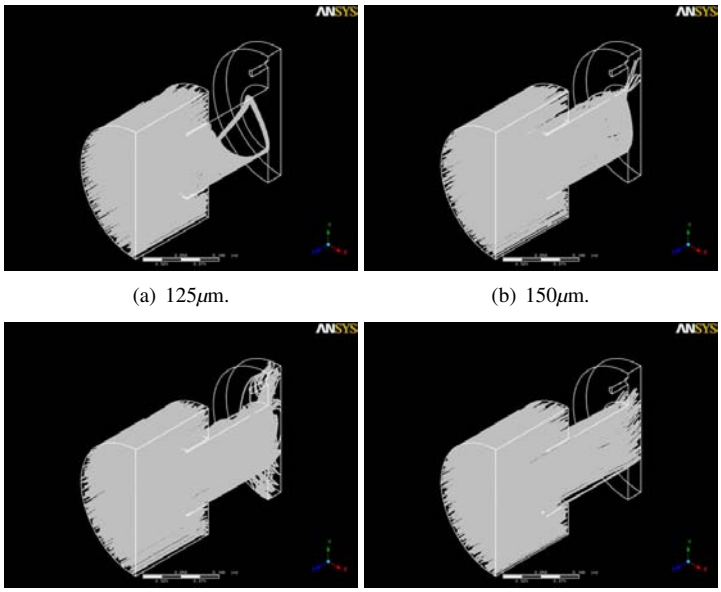

(a) 125μm. (b) 150μm.

(c) 175μm. (d) 200μm.

Figure 3.1: CFD results for 1 inlet windows purging system with different drop diameters. In each of the figures droplets enter from the left and meet the flow of nitrogen gas originating from the inlet in the window cavity to the right.

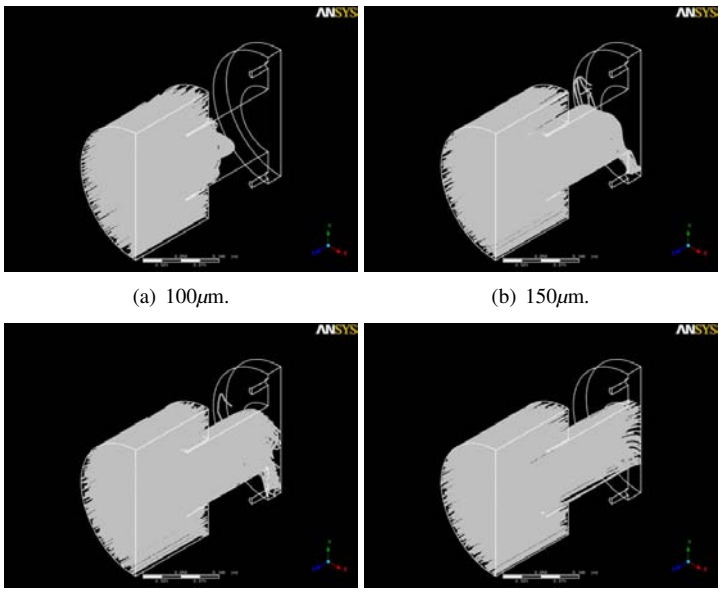

(a) 100μm. (b) 150μm.

(c) 175μm. (d) 200μm.

Figure 3.2: CFD results for 2 inlet windows purging system with different drop diameters. In each of the figures droplets enter from the left and meet the flow of nitrogen gas originating from the inlet in the window cavity to the right.

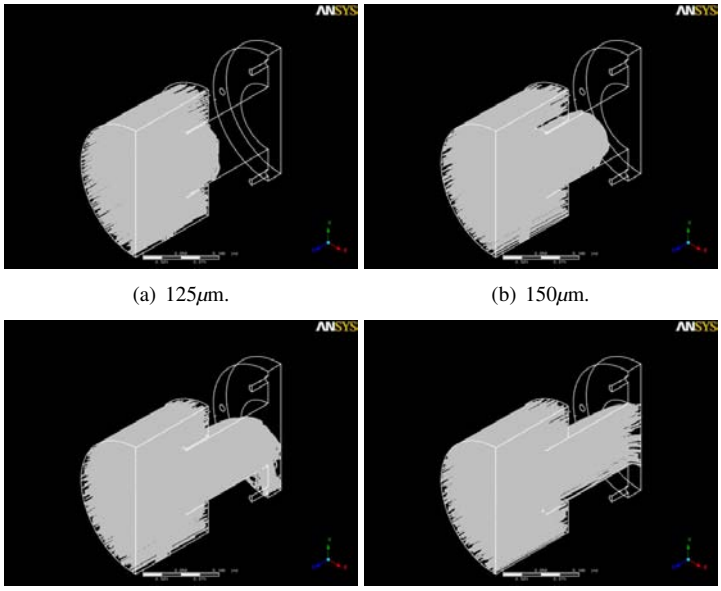

(a) 125μm. (b) 150μm.

(c) 175μm. (d) 200μm.

Figure 3.3: CFD results for 4 inlet windows purging system with different drop diameters. In each of the figures droplets enter from the left and meet the flow of nitrogen gas originating from the inlet in the window cavity to the right.

3.1.2 Experimental results

In figure 3.4 pictures of the results from the experiments are presented. In case 1 and 2 where the nozzle is in the lower position with a water flow rate of 9 l_n/min for case 1 and 13.8 l_n/min for case 2 a fairly low amount of droplets reach the window. For case 3 and 4 where the nozzle is in the higher position and the liquid flow rate is 9 l_n/min and 13.7 l_n/min respectively, the number of droplets that reach the windows is higher than for the cases with the nozzle in the lower position. In all cases (1-4) water ended up in the outer part of the tube and after awhile the water gets into the cavity between the glass and the purging system and contaminates the glass with droplets. In case 5 and 6 with the liquid flow rate of 9.0 l_n/min and 14.1 l_n/min the purging system is turned so that the inlet for the nitrogen gas is in the lower part of the window cavity. In these two cases it can clearly be seen that the purging system works better for these cases when the inlet is in the lower part of the cavity compared to the opposite configuration.

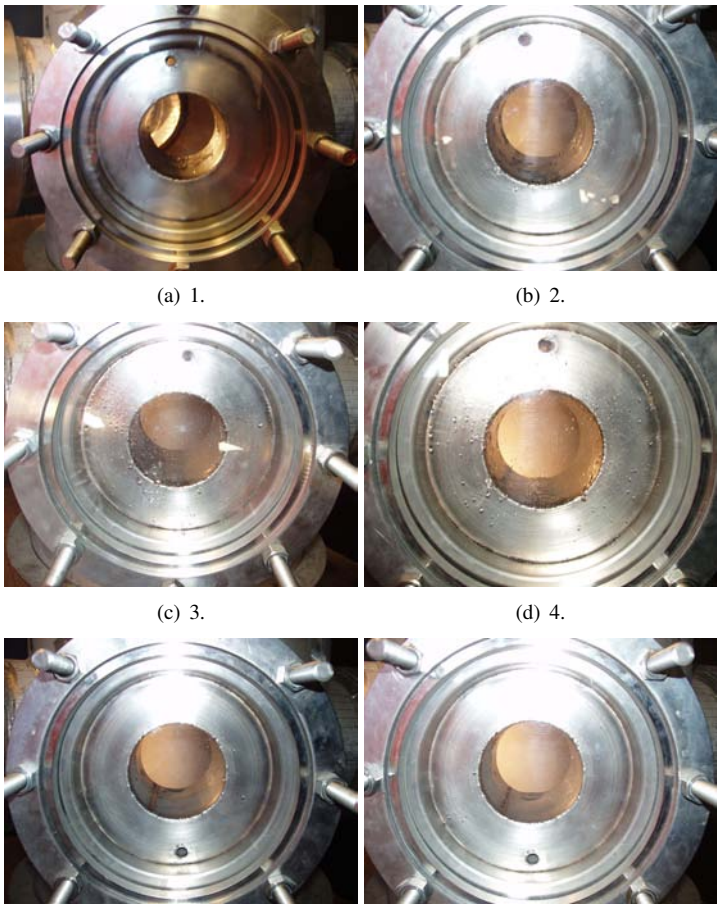

(a) 1. (b) 2.

(c) 3. (d) 4.

(e) 5. (f) 6.

Figure 3.4: Experimental test results for windows purging system.

3.2 Water spray visualisation

In this section the results from the single water spray visualisation are presented. The water flow rate was 4.9 l_n/min and the nitrogen gas flow rate was 441 l_n/min. In figure 3.5 a picture of the atomisation process near the nozzle is shown (The nozzle end can be seen in the left of the picture). The water jet moves from left to right in the picture but in reality the flow is vertical instead of horizontal. It can be seen that the flow is very turbulent and starts to break up into droplets at the right end of the image. For this case a typical velocity at the nozzle is 20 m/s. The velocity was calculated from a series of pictures where a droplet was able to be followed. 2 dm downstream from the nozzle (figure 3.6) the spray has broken up to spherical droplets as it can be seen in the figure as dark spots that show the contours of the water droplets. A typical velocity 2 dm down from the nozzle was 20 m/s. In figure 3.7 some examples on droplet shapes are shown.

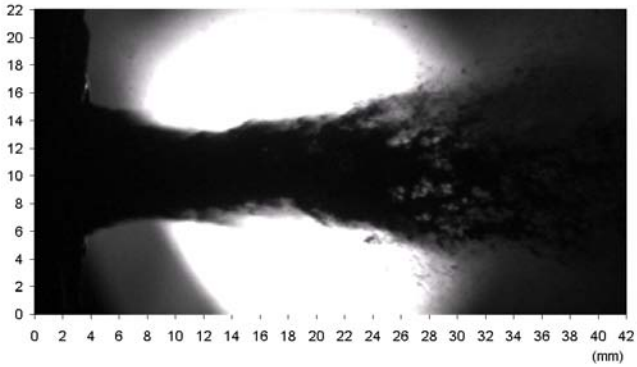

Figure 3.5: Water spray atomisation at the nozzle exit.

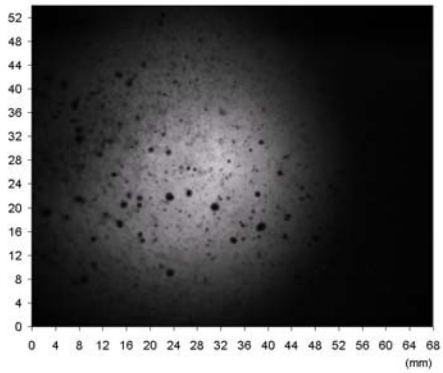

Figure 3.6: Water spray atomisation 2 dm below the nozzle exit.

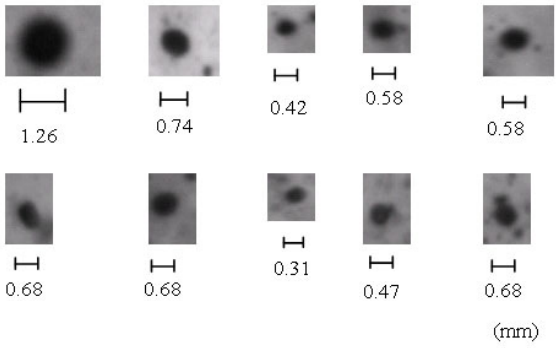

Figure 3.7: Examples of water spray atomisation droplets.

3.3 Black liquor spray visualisation

In this section the results from the different cases of black liquor spray visualisations (see table 2.7) are presented. For some cases both pictures at the nozzle and 2 dm downstream from the nozzle are presented. However, for some of the cases only pictures at the nozzle or 2 dm downstream from the nozzle are presented. The last three cases show on how the black liquor sprays behave under elevated ambient pressure.

3.3.1 Case 1

In case 1 the black liquor flow rate was 4.9 l_n/min and the nitrogen gas flow rate was 441 l_n/min . The temperature of the liquid was about 102°C and had 75.2 percent dry solid. The momentum flux ratio was 60 for this case assuming a choked flow at the gas exit. In figure 3.8 it can be seen that the flow was very turbulent and has broken up into ligaments and droplets in the right end of the picture. It was also found that the flow of black liquor was fluctuating, which can be seen in figure 3.8 where it starts to build up a chunk of black liquor (figure 3.8(a)) and then when the chunk is quite large it break and release the chunk (figure 3.8(b)). After that, in figure 3.8(c), it is very little black liquor but it starts to build up a chunk again. The interval of this sequence is about 0.014 seconds. Finally, for this case a typical velocity near the nozzle exit was found to be 18 m/s.

3.3.2 Case 2

In this case the nitrogen gas flow was increased to 588 l_n/min, which resulted in a momentum flux ratio of 80. The other variables were like in the first case. The result for this case is similar to the first case but the interval for the chunk build up and break up is harder to determine. It ranges from 0.010 to 0.015 seconds. From a series of pictures it was also seen that the black liquor got a higher velocity in this case compared to case 1 and a typical velocity was here about 23 m/s near the nozzle. In figure 3.9 a picture of the results from this case is presented were it can be seen how the black liquor breaks up into ligaments and droplets in right end of the picture.

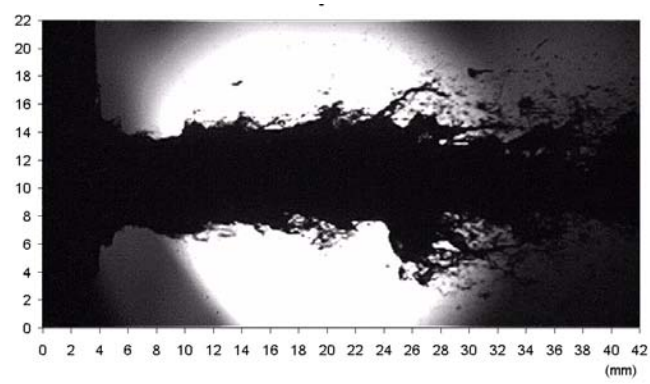

(a) Before breakup

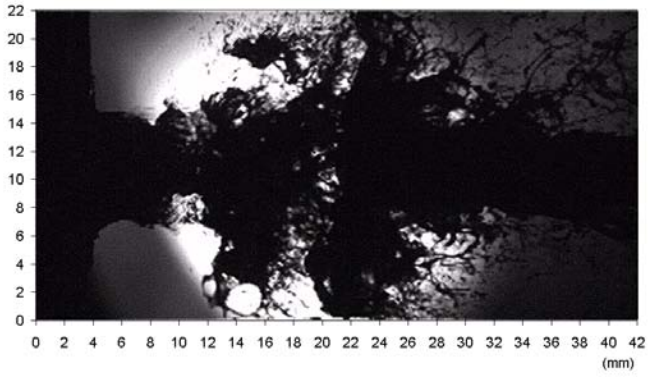

(b) Breakup

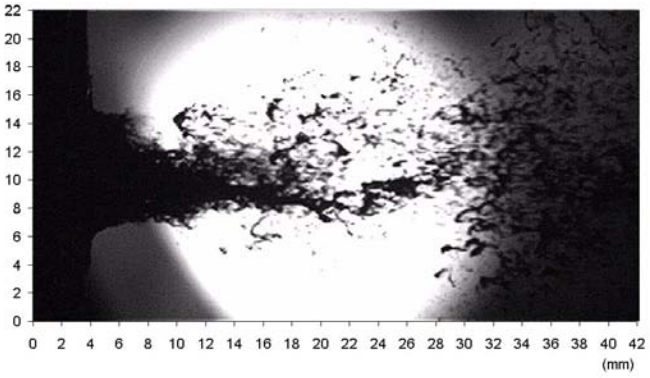

(c) After breakup

Figure 3.8: Black liquor spray atomisation at the nozzle exit for case 1.

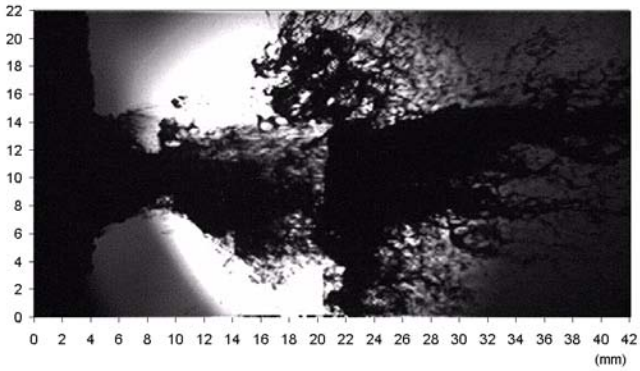

Figure 3.9: Black liquor spray atomisation at the nozzle exit for case 2.

3.3.3 Case 3

For case 3 the nitrogen gas flow was increased to 735 l_n/min, which increased the momentum flux ratio to 100. The other variables were the same as for the earlier cases. In this case pictures are taken at the nozzle but also 2 dm downstream from the nozzle to visualise how the black liquor spray has formed. In figure 3.10 it can be seen that the flow is similar as the earlier cases but with higher black liquor speed due to the increased nitrogen flow rate. In this case a typical velocity was 27 m/s. The chunk buildup and breakup was more random and the interval was shorter, ranging from 0.006 to 0.008 seconds. The results 2 dm below the nozzle are presented in figure 3.12 and shows that the black liquor has broken up into ligament and non spherical droplets. In some of the pictures, e.g. figure 3.12(b), a coarse spray appears and in others, e.g. 3.12(c), a more dense black liquor spray is observed, which is due to the fluctuation at the nozzle. In figure 3.11 some examples of different droplets shapes are shown. Here it can be seen that the shape of the droplets in the resulting black liquor spray are nearly spherical in some cases while others are in forms of long ligaments. Also, some of the droplets were more like chunks of black liquor. For this case 2 dm below the nozzle a typical velocity was found to be 27 m/s.

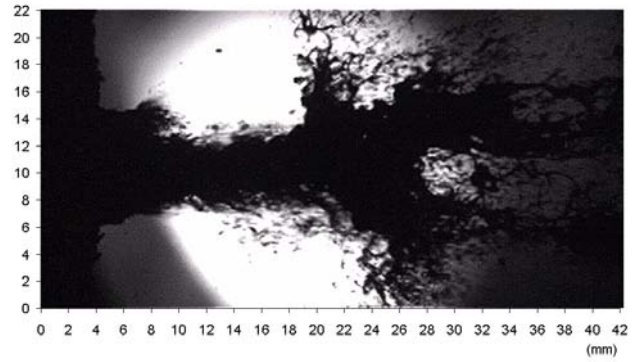

Figure 3.10: Black liquor spray atomisation at the nozzle exit for case 3.

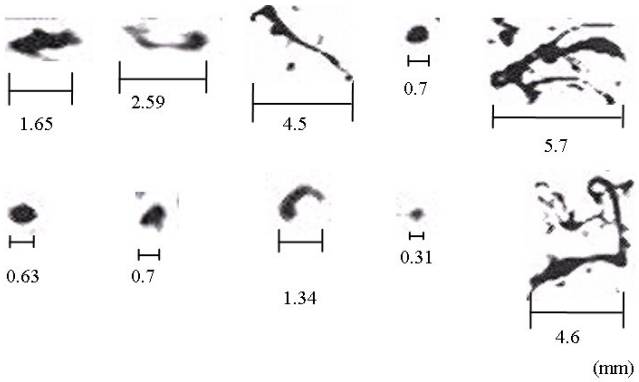

Figure 3.11: Examples of droplets shape of black liquor in case 3.

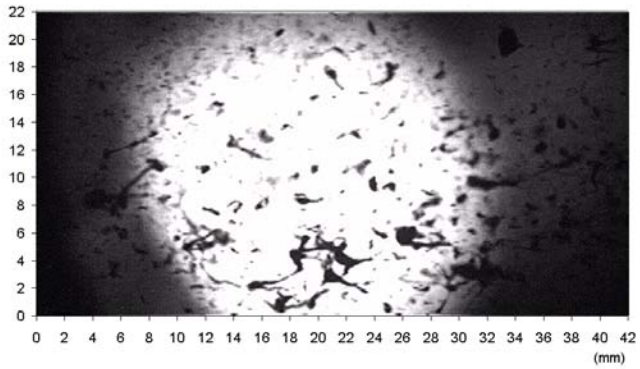

(a)

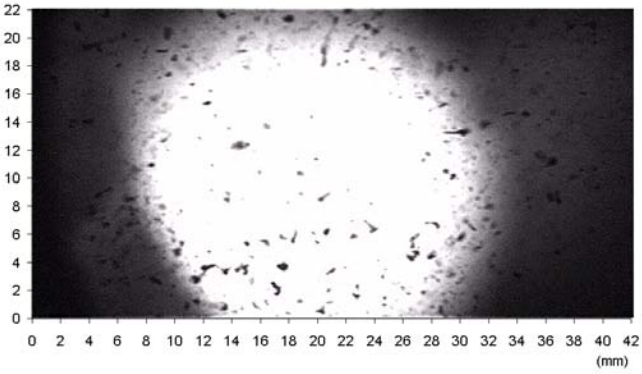

(b)

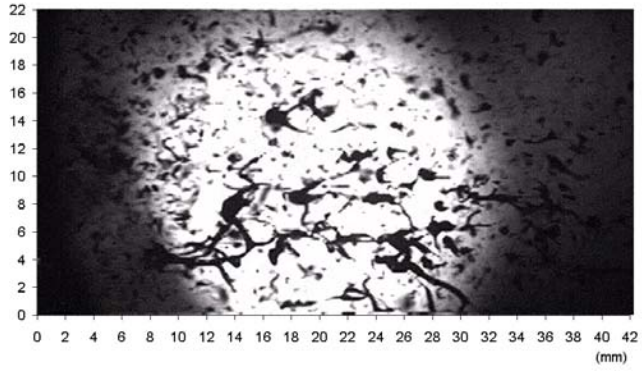

(c)

Figure 3.12: Three different pictures the resulting black liquor spray 2 dm below the nozzle exit for case 3.

3.3.4 Case 4 to 6

In this section the results for case 4 to 6 are presented. In these cases the black liquor flow is higher than in case 1 to 3 and also the nitrogen gas flow rate. The black liquor flow rate was 7.3 l_n/min and the nitrogen gas flow rate was 992 l_n/min for case 4, 1322 l_n/min for case 5 and 1652 l_n/min for case 6. These conditions resulted in a momentum flux ratio of 60 for case 4, 80 for case 5 and 100 for case 6. In figure 3.15 the results at the nozzle are presented for each of the current cases. It can be seen that these cases look much like the earlier cases but with a higher velocity of the black liquor. For case 4 the typical velocity was about 30 m/s, for case 5 about 34 m/s and for case 6 about 38 m/s. The velocities near the nozzle in these cases were hard to determine since the velocity of the black liquor was too high in order to be able to be freezed with the current camera satisfying. For these cases it could also be seen that the black liquor fluctuate as in case 1 to 3, but here it was harder to determine the period of the fluctuation. In figure 3.13 the results 2 dm below the nozzle are presented for case 6. It was found here that a typical velocity is about 50 m/s for a droplet and compared to case 3 the droplet size seems to be smaller. In figure 3.14 some examples of different droplet shapes are shown and it can be seen that droplets are both in form of ligaments and nearly spherical.

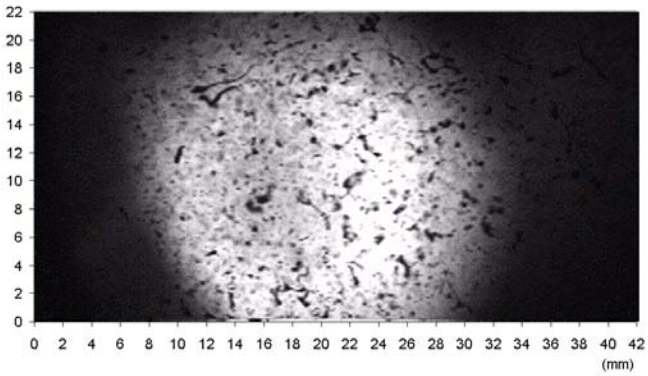

Figure 3.13: Black liquor spray atomisation 2 dm below the nozzle exit for case 6.

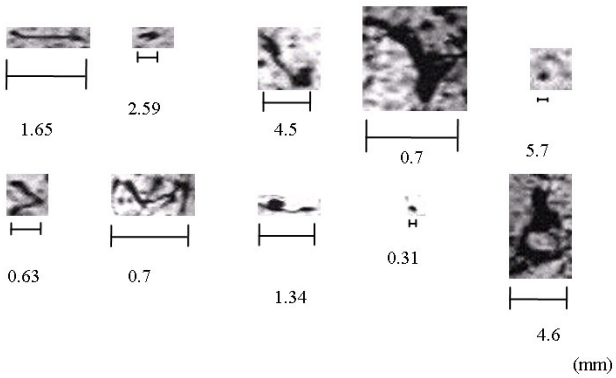

Figure 3.14: Examples of droplet shapes in the resulting black liquor spray in case 6.

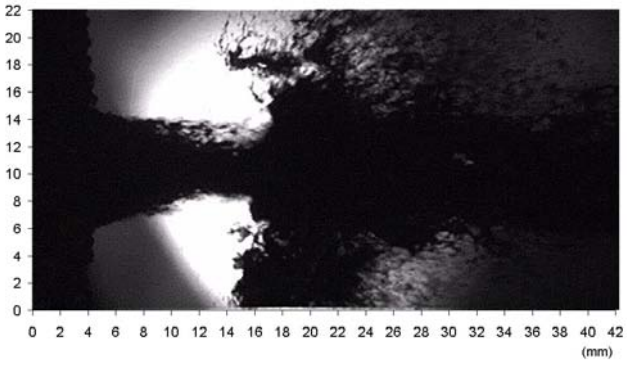

(a) Case 4

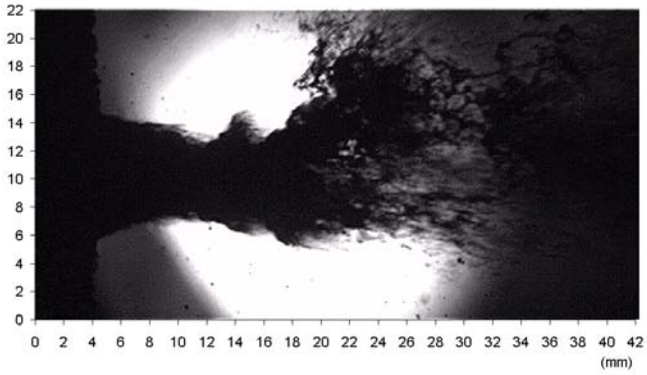

(b) Case 5

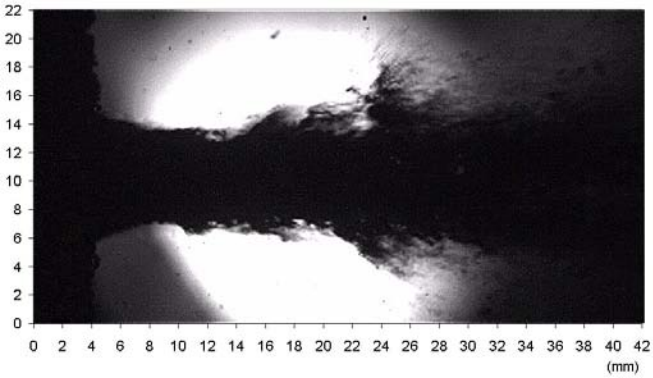

(c) Case 6

Figure 3.15: Black liquor spray atomisation at the nozzle exit for case 4 to 6.

3.3.5 Case 7 and 8

In these cases the temperature was raised to about 112 °C for the black liquor. However the dry solids content was decreased to 70.2 % dry solids. The black liquor flow was 4.9 l_n/min and the nitrogen gas flow was 441 l_n/min for case 7 and 735 $l_n/min$for case 8. These flow rates were the same as in case 1 and 2. In figure 3.16 the results for case 7 are presented and in figure 3.17 the results for case 8 are presented. From these two figures it can clearly be seen that the droplet sizes decrease when the momentum flux ratio is increased. For case 7 a typical velocity was found to be 14 m/s and for case 8 a typical velocity was 22 m/s. Furthermore, some example droplets can be found in figure 3.18 for case 7 and in figure 3.19 for case 8. The size of the droplets are about the same for case 8 as was found for case 3 having the same flow rates. However, it should be noted that the temperature was increased for case 8 and the black liquor had a lower percent dry solids. Further the droplet shapes was as irregular as in the earlier cases.

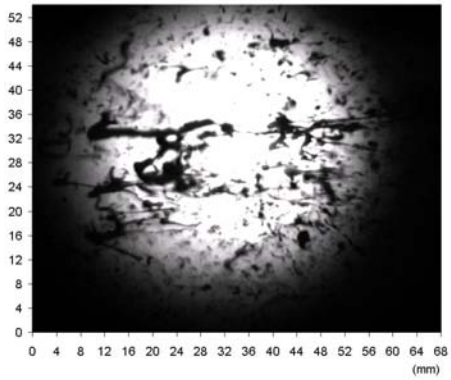

Figure 3.16: Black liquor spray atomisation 2 dm below the nozzle exit for case 7.

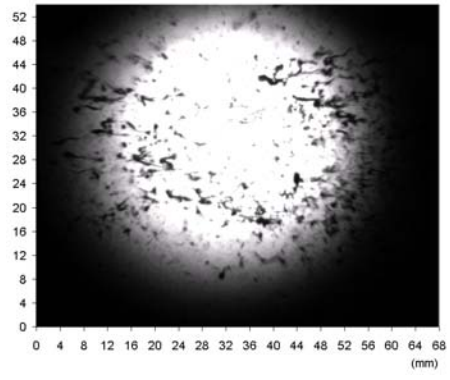

Figure 3.17: Black liquor spray atomisation 2 dm below the nozzle exit for case 8.

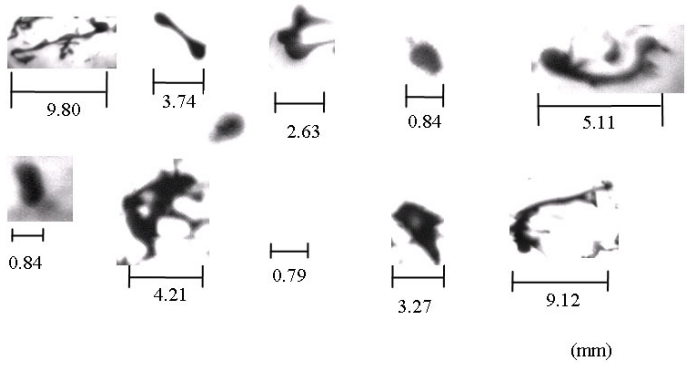

Figure 3.18: Examples of droplet shapes of black liquor in case 7.

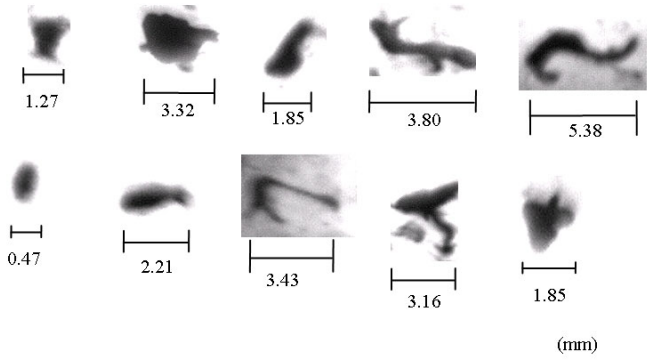

Figure 3.19: Examples of droplet shapes of black liquor in case 8.

3.3.6 Case 9 and 10

In these cases the black liquor flow was 7.3 l_n/min and the nitrogen gas flow was 992 l_n/min (M=60) for case 9 and 1652 l_n/min (M=100) for case 10. Case 9 and 10 had the same black liquor flow and nitrogen gas flow as case 4 and 6 but the temperature was raised to 112 °C for these cases. However, the percent dry solid was decreased to 70.2% dry solids. In figure 3.20 and 3.21 the results for case 9 and 10 are shown, respectively. Compared to case 7 and 8 it can clearly be seen that the droplet size has decreased. Furthermore, comparing case 9 to case 10 shows that the droplet size has decreased like in the earlier cases with an increase of the momentum flux ratio. A typical velocity for case 9 was 20 m/s and for case 10 a typical velocity was 36 m/s. Finally, in figure 3.22 and 3.23 some examples of droplets are shown for these cases showing that some long ligaments are present, particularly in case 9.

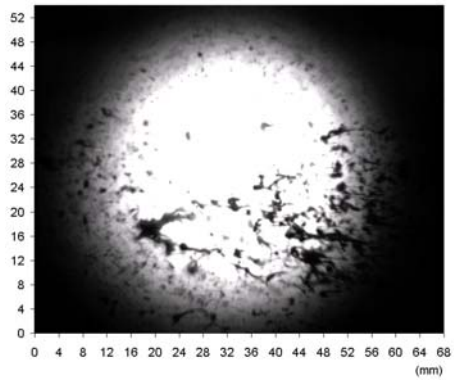

Figure 3.20: Black liquor spray atomisation 2 dm below the nozzle exit for case 9.

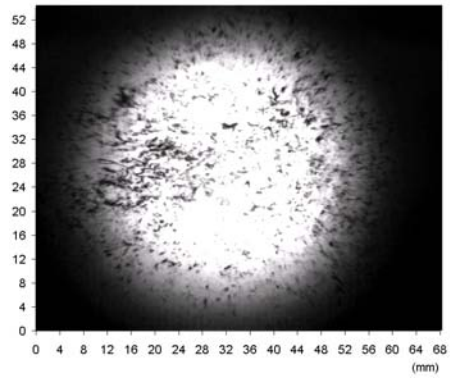

Figure 3.21: Black liquor spray atomisation 2 dm below the nozzle exit for case 10.

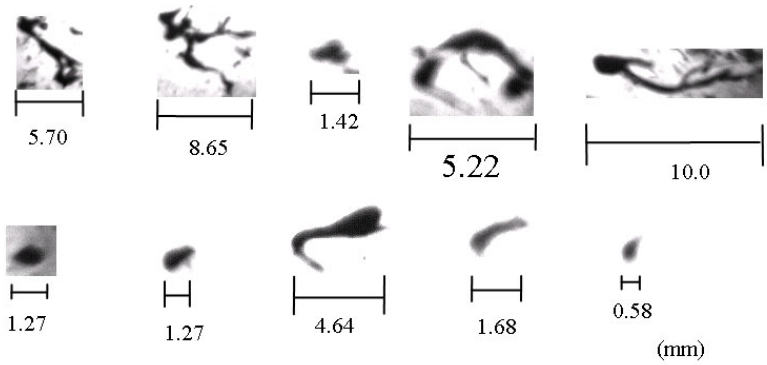

Figure 3.22: Examples of droplet shapes of black liquor in case 9.

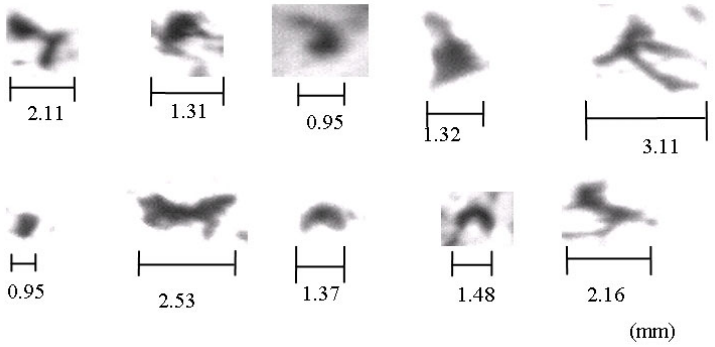

Figure 3.23: Examples of droplet shapes of black liquor in case 10.

3.3.7 Case 11 to 13

In case 11 to 13 the ambient pressure into which the black liquor is sprayed is increased. For case 11 the absolute pressure was 5 bar and for the two other cases 10 bar. Case 11 and 12 have the same flow rates as in case 10 (7.3 l_n/min of black liquor flow and 1652 l_n/min of nitrogen gas). The resulting momentum flux ratio in these cases will decrease compared to case 10 due the compressible of the nitrogen gas. In case 13 the nitrogen gas flow rate was increased to 2140 l_n/min to obtain a momentum flux ratio of 60. The temperature of the black liquor in these cases was 112°C and 70.2% dry solids. In figure 3.24 two pictures from case 11 are presented and in figure 3.25 and figure 3.26 for case 12 and 13 respectively. In figure 3.24 it can be seen that the black liquor looks more like a cloud of small droplets compared to the earlier cases, but still some larger droplets and ligaments can also be found. The results for case 12 and 13 are very similar to case 11 and it is very hard do determine any differences in the size of the droplets between these cases. The typical velocities of the droplets are 27 m/s for case 11, 17 m/s for case 12 and 24 m/s for case 13. Regarding the velocity, case 12 compared to case 11 shows that the velocity is decreased with higher pressure. In figure 3.27,3.28 and 3.29 some examples of droplet shapes are presented for these cases.

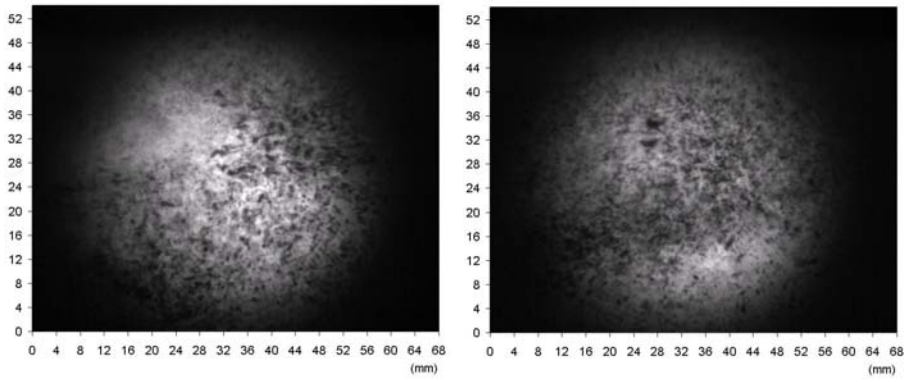

(a) (b)

Figure 3.24: Two pictures at different ocassions of the black liquor spray atomisation 2 dm below the nozzle exit for case 11.

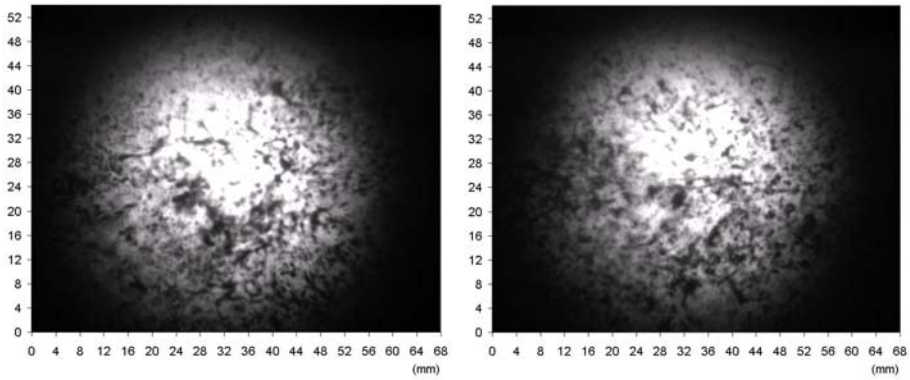

Figure 3.25: Two pictures at different ocassions of the black liquor spray atomisation 2 dm below the nozzle exit for case 12.

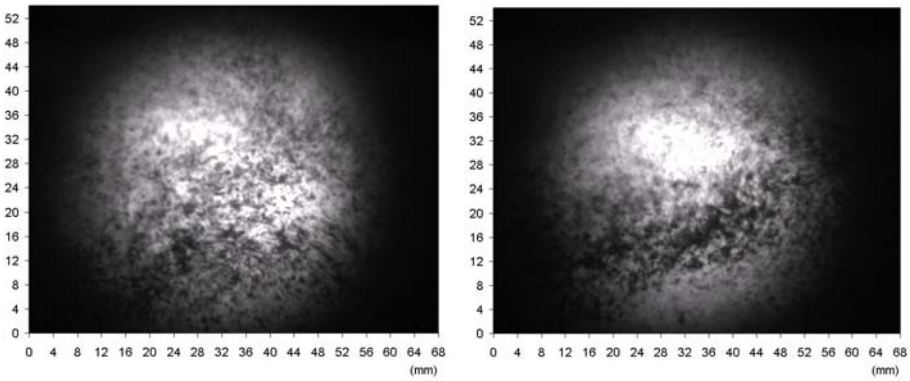

Figure 3.26: Two pictures at different ocassions of the black liquor spray atomisation 2 dm below the nozzle exit for case 13.

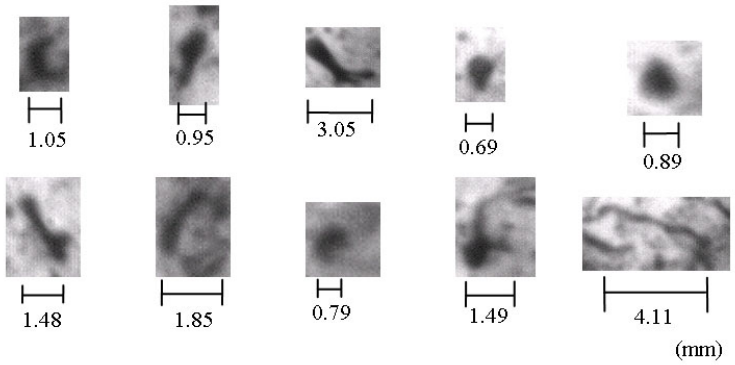

Figure 3.27: Examples of droplet shapes of black liquor in case 11.

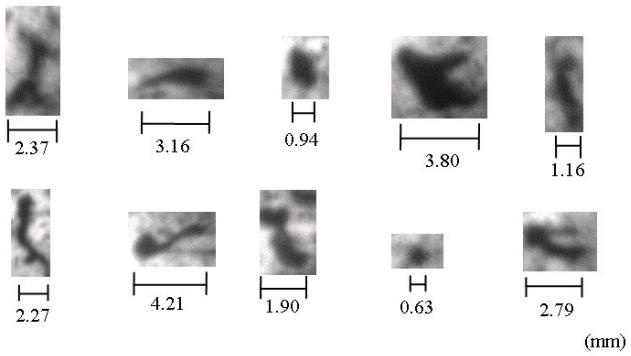

Figure 3.28: Examples of droplet shapes of black liquor in case 12.

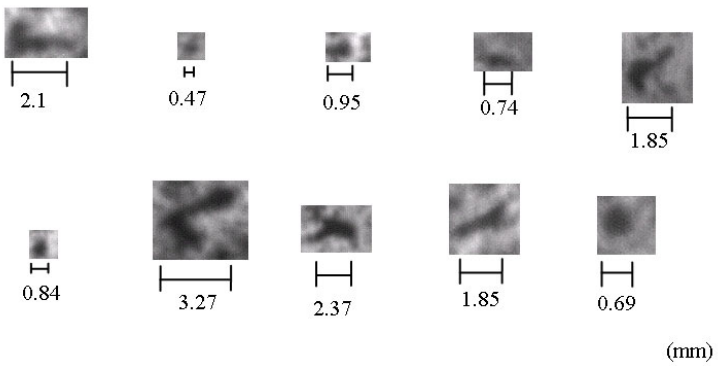

Figure 3.29: Examples of droplet shapes of black liquor in case 13.

Chapter 4

Discussion and conclusions

4.1 Experimental setup

The current window purging system has been proven to work both for water and black liquor. For black liquor it works even better than for water because the black liquor does not re–circulate up towards the top in same way as water does in the pressure vessel. The window purging system is easily mounted with three screws to fix the system into the optical access port. The CFD simulations show that the purging system protects the window against small droplets. The CFD model used in the simulations can be used to further optimise and improve the purging system. The current work also proved that the system works at pressurised conditions.

To pump the black liquor into the spray test rig two pumps were used. A lobe pump on the pressure side and an eccentric screw pump to feed the lobe pump on the suction side. Tests with only the use of the lobe pump show that the pump cavitates. By using the eccentric screw pump to build up the pressure on the suction side of the lobe pump the cavitation is prevented. The lobe pump must still be used because it can handle larger pressure on the pressure side (15 bar instead of 6 bar for the eccentric screw pump).

When heating the black liquor it was first heated with an oil drum heater in the storage vessel to about 105 °C. In order to heat the black liquor to about 115 °C a peak heater was constructed. The peak heater was able to heat the black liquor to about 115 °C before the liquor started to boil. To heat the black liquor above this temperature the black liquor must be heated under pressure. This may be done with some sort of heat exchanger after the lobe pump.

To be able to control the flow of nitrogen gas to the spray test rig a gas heater was installed that could heat the gas about 20 °C. One problem with the nitrogen heater is that it is currently controlled with a thermostat with on and off regulation. Because of this the temperature of the gas is hard to maintain constant at 20 °C. Some sort of new control system should be installed in order to give better regulation. Finally, two mass flow controllers were installed to control the gas flow. With the controllers it was very easy to control the gas flow rate to the nozzle.

4.2 Spray visualisation

4.2.1 Water and nitrogen

The water spray visualisation shows that the droplets in the resulting water sprays are spherical. The droplet sizes are spread over a wide range and it is hard to determine the size of the smallest droplets but it may be as small as a few microns. The largest droplets observed are more than 1 millimetre in diameter. To be able to get better resolution for the smaller droplets a zoom objective with higher magnification could be used. In the water run it was also observed that the water started to re–circulate in the pressure vessel causing a cloud of small water drops in the top of the vessel.

4.2.2 Black liquor and nitrogen

The black liquor spray visualisations show that the black liquor flow at the nozzle appears to fluctuate. This fluctuation may be caused by an unstable flow rate of the black liquor from the pump or due to an in–stationary atomisation mechanism caused by the high viscosity of the black liquor building up a chunk of black liquor before it breaks up by atomisation. Based on the observation that the fluctuations are random for different cases they cannot be directly related to the pumps number of revolutions. To bring more understanding in this issue further investigation is needed.
Even though some of the droplets are nearly spherical the shape of most of the black liquor droplets are non spherical and some look more like ligaments. The size of the largest droplets are several mm for every case. This can be explained by the nozzle used in this work is not an optimised nozzle for black liquor gasification. From the results it can furthermore be shown that the size of droplets decreases with increasing load of atomisation gas. Compared with the work done by Mackrory [13] the droplets that are shaped like ligaments in this work seem to be shorter compared to the ligaments in that work. This can be explained by the higher momentum flux ratio used in the current work. From the result, the conclusion is that the drop sizes reduced significantly with an increase in the moment flux ratio. Furthermore, the droplet velocities increase with increased moment flux ratio, as expected.

Influence of temperature and dry solids content

Based on the few results with varying temperature, the results show very little dependence on temperature in the atomisation process. In the experiment the temperature was raised from 105 °C to 115 °C and at the same time the dry solid was lower in the cases with the higher temperature.
Since the temperature and dry solids content affect the viscosity, no clear change in the spray due to changes in viscosity was observed, the size of droplets is about the same. However, further investigations are needed in order to be able to draw conclusions with better control concerning the effects of temperature and dry solids content. Especially it would be of great interest to raise the temperature significantly above the atmospheric boiling point. Miikkulainen [26] showed that the drop sizes decrease when the temperature is increased above the atmospheric boiling point.

Influence of pressure

Under the influence of elevated ambient pressure the behaviour of black liquor spray changed. With increased pressure it appears as if the spray cloud contracts and the black liquor looks more like a dense cloud of small droplets than larger more coarsely distributed droplets in the atmospheric cases. Still some ligaments and non spherical droplets are present. Most of the black liquor droplets are very small and it is hard to distinguish individual droplets in the dense cloud of black liquor droplets. The general observation is that the droplet sizes appears to be smaller under pressurised conditions. Any differences between the cases are hard to find. In order to be able to see the shape of the smaller droplets a lens with higher magnification is recommended. From the picture it can furthermore be seen that the light penetrates less efficiently through the spray. From this the conclusion that the spray is denser under pressure can be made. It should however be mentioned that the general observation of denser spray may be an effect from a possible recirculation in the pressure vessel. The velocity of the droplets decrease when the ambient pressure increases as expected since the velocity of the gas will decrease and the black liquor are sprayed into an environment with a higher gas density.

Chapter 5

Future work

Below follows some recommendations for possible future work within the current subject.

- Perform visualisations on black liquor spray atomisation with different nozzles, e.g. nozzles that have been found to work well in the DP–1 gasifier.
- Install a heat exchanger after the lobe pump to be able to heat the black liquor above the atmospheric boiling point temperature when the black liquor is under pressure.
- Develop a system of water nozzles inside the pressure vessel to be able to clean the vessel easily.
- Construct a lifting device that is able to easily lift of the top cap of the pressure vessel.
- Develop an image analysis program to perform image analyses of the pictures. For example, determine the size of the droplets or the velocities in the sprays.

Bibliography

[1] Skogsindustrin. Skogsindustrin en faktasamling 2006. Technical report, 2006.

[2] Energimyndigheten. Energy in sweden. facts and figures. Technical report, 2007.

[3] Marklund M. *Pressurized Entrained-flow High Temperature Black Liquor Gasification*. PhD thesis, Department of Applied Physics and Mechanical Engineering, Division of Fluid Mechanics, Luleå University of Technology, 2006.

[4] Grace T.M. *Chemical Recovery in the Alkaline Pulping Processes 3ed*, chapter Chemical Recovery Process Chemistry, pages 57–78. Atlanta: TAPPI press, 1992.

[5] Hupa M., Backman R., and Frederick W.J. Black liquor combustion properties. In *International Conference Baltic Sea*. Finnish Recovery Boiler Committee, 1994.

[6] Forssén M, Backman R, Wallén J, and Hupa M. Flygaskans sammansättning och nedsmutsande tendens i sodapannan. Technical report, Värmeforsk service AB, Stockholm, 2000.

[7] Axegård P. Kretsloppsanpassad massafabrik–slutrapport. Technical report, KAM 1 1996-1999, KAM–Rapport A31, Striftelsen för Miljöstrategiosk forskning, 1999.

[8] Lefebvre Arthur H. *Atomization and Sprays*. Taylor and Francis, 1989.

[9] Adams T.N. and Frederick W.J. Kraft recovery boiler physical and chemical process. Technical report, The American Paper Institute, Inc. New York, 1988.

[10] Soderhjelm L. and Koivuniemi U. Recent developments in black liquor analysis. Technical report, Black Liquor Recovery Boiler Symposium, 1982.

[11] Soderhjelm L. Characterization of kraft black liquor with respect to evaporation and combustion. Technical report, The finnish pulp and paper research institute, Helsinki, 1988.

[12] Mackrory Andrew J. and Baxter Larry L. Characteristics of black liquor sprays from gas–assisted atomizers in high temperature environments. In *Proc. International Chemical Recovery Conference May 29 – June 1*, 2007.

[13] Mackrory A.J. Characterization of black liqour sprays for application to entrained-flow processes. Master thesis, Department of Mechanical Engineering, Brigham Young University, 2006.

[14] Loebker D.W. and H.J. Empie. Independently controlled drop size in black liquor sprays to the kraft recovery boiler using effervescent atomization. Technical report, Institute of Paper Science and Technology Atlanta, Georgia, 1999.

[15] D Karlsson and S Westerlund. A unique pressurized spray test facility for optimization of black liquor gasification. Master thesis, Department of Applied Physics and Mechanical Engineering, Division of Fluid Mechanics, Luleå University of Technology, 2006.

[16] Paisley P.L. What constitutes high speed photography? *OE Reports*, November 1993.

[17] Sidney F.Ray. *High Speed Photography and Photonics*. SPIE PRESS, 2002.

[18] Lavision, Dec 2007. http://www.lavision.de/.

[19] Dantec dynamics, Dec 2007. http://www.dantecdynamics.com/.

[20] Brooks instrument. *Installation and Operation Manual. Brooks Smart Series (TMF)*.

[21] A flow measurement primer - thermal mass flow meters., Dec 2007. http://www.crossinstrumentation.com/ga/mfg/Flow/tmf_meters.htm.

[22] How the progressing cavity pump works., Dec 2007. http://www.engineering-talk.com/news/net/net103.html.

[23] JABSCO. *HyLine and Ultime Lobe Pumps Technical Data Sheet*.

[24] ELIZ PLZEN a.s. *Design, Assembly and Service Manual. Induction flow meter FLONET FN20XX*.

[25] Dedocool product catalog coolh, Dec 2007. http://www.dedotec.com/dedolight/.

[26] Miikkulainen P. *Experiments on black liqour spray formation in recovery boiler furnaces*. PhD thesis, Department of Mechanical Engineering, Helsinki University of Technology, 2006.